Status and Drivers of Dissolved Oxygen in Regulated Rivers

Marco Cunico

Master's Thesis • 60 credits
Swedish University of Agricultural Sciences, SLU
Faculty of Forest Science, Department of Wildlife, Fish, and Environmental Studies
Conservation and Management of Fish and Wildlife
Examensarbete / SLU, Institutionen för vilt, fisk och miljö
2025:14
Umeå 2025

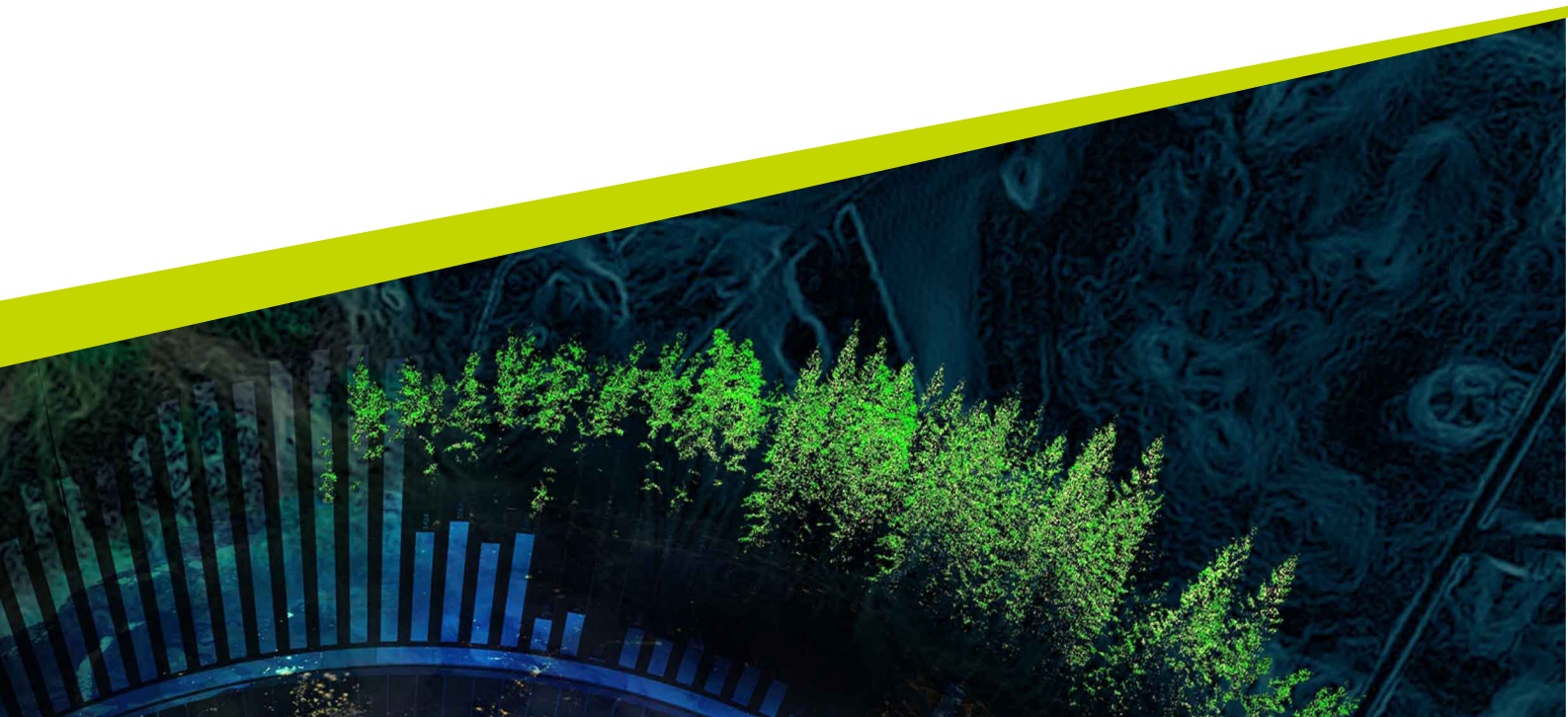

Status and Drivers of Dissolved Oxygen in Regulated Rivers

Marco Cunico

Supervisor:	**Navinder J Singh, SLU, Department of Wildlife, Fish, and Environmental Studies**
Assistant supervisor:	Åsa Widén, SLU, Department of Wildlife, Fish, and Environmental Studies
Assistant supervisor:	Jani Ahonen, SLU, Department of Wildlife, Fish, and Environmental Studies
Examiner:	Frauke Ecke, University of Helsinki

Credits:	60 Credits
Level:	Master, A2E
Course title:	Master Thesis in Biology
Course code:	EX0970
Programme/education:	Conservation and Management of Fish and Wildlife
Course coordinating dept:	Department of Wildlife, Fish, and Environmental Studies
Place of publication:	Umea, Sweden
Year of publication:	2025
Title of series:	Examensarbete / SLU, Institutionen för vilt, fisk och miljö
Part Number:	2025:14

Keywords:	Dissolved oxygen (DO), Hypoxia, Flow regulation, Hydropeaking, Generalized Additive Model (GAM), Water Framework Directive (WDF), Ecological potential

Swedish University of Agricultural Sciences
Forest Science
Wildlife, Fish, and Environmental Studies

Abstract

Oxygen is critical for life and plays a pivotal role in ecosystem functioning supporting both respiration and biogeochemical cycles. In natural aquatic environments its availability is primarily regulated by photosynthesis and aeration. Water flow and its natural regime influences community composition both directly and indirectly. While Hydropower provides a renewable energy source, water regulation poses a significant threat to the ecological integrity of regulated rivers. In response European Water Framework Directive (WDF) emphasizes the importance of conserving and restoring the ecological potential of heavily modified water bodies (HMWBs). In this study I investigate the temporal and spatial variation of Dissolved oxygen (DO) at an hourly resolution in three regulated rivers (Luleälven, Umeälven, Ljungan) and two free-flowing rivers (Vindelälven, Piteälven) in central and northern Sweden over summer months using Generalized Additive Model (GAM). I found significantly lower levels of mean DO in regulated rivers with a higher variability, and occurrence of severe hypoxia (< 3mg/l) and anoxia (0mg/l) at times. Furthermore, DO showed strong correlation with time of the day, hourly discharge, and duration of zero flow in regulated river. Thus, I emphasize the need for a high spatial and temporal monitoring of DO in regulated rivers to enable accurate and early detection of harmful hypoxic events in HMWBs, Additionally, I argue the importance of including ecological limits and requirements in hydropeaking schemes, along with the strict enforcement of environmental flows (e-Flow) improving sustainability of hydroelectric energy production.

Keywords: Dissolved oxygen (DO), Hypoxia, Flow regulation, Hydropeaking, Generalized Additive Model (GAM), Water Framework Directive (WDF), Ecological potential

Acknowledgments

I would like to thank my supervisors, Navinder Singh (SLU) and Åsa Widen, for their advice, support, and guidance throughout the course of this thesis.

I also extend my thanks to the EU-interreg project RE-HYDRO, for the financial support and the collaborative environment provided. In particular, I am grateful to Ritesh Patro (University of Oulu) for his support and contributions during this project. Special thanks go to Jani Ahonen (SLU) for his guidance in the field and for sharing his deep knowledge of river restoration practices. I would also like to thank Roland Jansson, Birgitta Malm-Renöfält (Umeå University), and the Ekofall project for providing part of the oxygen loggers and for their valuable insights into river regulation, hydropower, and related ecological considerations. Furthermore, I am grateful to the collaborating hydropower companies -Vattenfall, Uniper, and Statkraft -for the trust and the flow data provided which were crucial to this research.

Table of contents

List of tables

List of figures

Abbreviations

Abbreviation	Description
CRS	Coordinate Reference Systems
DO	Dissolved Oxygen
EQSD	European Quality Standard Directive
GPS	Global Positioning System
HM	Heavily Modified
HMWBs	Heavily Modified Water Bodies
HP	Hydropower Plant
Qmin	Minimum discharge turbine capacity
RBMPs	River Basin Management Plans
SLU	Swedish University of Agricultural Science
SMHI	Swedish Meteorological and Hydrological Institute
WDF	Water Framework Directive

1. Introduction

Oxygen is critical for all life and plays a pivotal role in the functioning of ecosystems.

In aquatic environments, molecular oxygen occurs as dissolved oxygen (DO) - O_2 molecules dispersed among water molecules in a free, unbound state that can be readily utilized by aquatic organisms through specialized structures such as gills. At atmospheric pressure, the dissolution of oxygen in water is primarily governed by temperature, as described by Henry's Law. Consequently, DO originates from two principal sources: diffusion from the atmosphere (aeration) and photosynthetic activity by aquatic plants and phytoplankton. The relative contribution of these sources varies between lotic and lentic ecosystems and across microsites, influenced by differences in water temperature, movement, stratification, surface area in contact with the atmosphere, light availability and others factors (Wetzel 2001; Cox 2003).

Furthermore, Dissolved oxygen exhibits daily cycle driven by the balance between photosynthesis and respiration, and seasonal variation due to temperature changes throughout the year. The dynamic balance between oxygen sources and sinks determines DO concentrations at specific times and locations, contributing to spatial and temporal heterogeneity within aquatic systems (Wetzel 2001; Fusi et al. 2023).

Rivers and streams can be viewed as the terrestrial phase of the water cycle, occurring when precipitation exceeds evapotranspiration and water begins to drain across various surfaces and flow paths within a catchment. These flow paths converge along lines of maximum slope, gradually increasing in discharge. Water may follow multiple flow paths with different travel times and may experience transient storage in features such as soils, snowpacks, glaciers, lakes, and wetlands (Stewardson et al. 2017). Together with other variables influencing the hydrological cycle -such as climate, geology, vegetation, and land use-this complex set of interactions shapes the flow regime of Rivers (Davie 2019a).

The flow regime can be decompose in five key components: Magnitude, Frequency, Duration, Timing, and Rate of change (Poff et al. 1997) which shape not only the physical structure and hydrological functioning of riverine ecosystems (Davie 2019a), but also the life history strategies, behaviours, and morphologies of aquatic and riparian species. Many plants and animals have evolved specific adaptations to exploit the natural variability and periodicity of flow regimes (Jansson et al. 2000; Lytle & Poff 2004), consequently, the flow regime influences community composition both directly and indirectly by mediating key ecological drivers such as water quality, energy availability, physical habitat structure, and biotic interactions. Thus, Water flow is a central determinant of ecological integrity in lotic systems and a foundational concept in River conservation and management (Poff & Allan 1995; Poff et al. 1997; BUNN & ARTHINGTON 2002; Lytle & Poff 2004; Poff & Zimmerman 2010)

Turbulence, water velocity, and mixing help regulate the diffusion of atmospheric oxygen into aquatic systems, while thermal patterns and stratification contribute to defining its spatial and temporal variability (Cox 2003; Stewardson et al. 2017; Davie 2019a). Fast-flowing, well-aerated reaches typically favour oxygen-sensitive species such as salmonids and certain macroinvertebrates, whereas slow-flowing conditions are often associated with species adapted to lower dissolved oxygen concentrations (Warren et al. 2015; Calapez et al. 2017). Again, flow and dissolved oxygen consistently emerge as key drivers of freshwater ecosystem structure and functioning, making them a central concern on River conservation, management, and restoration efforts (Diaz & Rosenberg 2008; Fusi et al. 2023).

The societal demand for renewable and flexible energy sources has driven the widespread development of hydropower systems and infrastructure globally. In 2022, hydropower accounted for 37% of the world's total installed renewable energy capacity and contributed 10% (283 TWh) of Europe's electricity output-led by Sweden, which produced approximately 69 TWh (*RENEWABLES 2023 GLOBAL STATUS REPORT* s.d.). Hydropower remains the dominant energy source in Sweden, representing around 40% of the national electricity mix in 2023, followed by nuclear (29%) and wind power (20%) (*Sweden - Countries & Regions* s.d.). A common operational strategy in modern hydropower systems is hydropeaking, a form of water regulation aimed at maximizing electricity generation in response to short-term fluctuations in energy demand and market prices. This often involves rapid and frequent changes in water flow and may result in abrupt discharge variations, including periods of zero flow in downstream river sections (Quaranta et al. 2021; Widén et al. 2021).

While hydropower offers a low-carbon energy alternative, its environmental impacts are increasingly recognized. Flow regulation, impoundment, and hydropeaking disrupt natural hydrological regimes, alter sediment transport, fragment aquatic habitats, and impair longitudinal and lateral connectivity with riparian zones. These operations can also degrade water quality, altering vertical connectivity and thermal regimes as well as changing ecosystem metabolism. For this reason water regulation for hydropower production might influence availability of dissolved oxygen (DO) (Dynesius & Nilsson 1994; Jansson et al. 2000; Nilsson et al. 2005; Poff & Zimmerman 2010; Stewardson et al. 2017; Grill et al. 2019; Widén et al. 2021; Parasiewicz et al. 2023). Hence, hydropower operations pose a serious challenge to the ecological integrity of regulated rivers and call for balanced management strategies that incorporate ecological considerations alongside energy and economic goals (Kallis et al. 2025).

In response to such challenges, the European Union issued the Water Framework Directive (WFD) (*Directive 2000/60/EC* 2000), a legislative framework which aim at protecting and restoring the ecological status of all costal, surface and ground water bodies across Europe. The WFD emphasizes the importance of maintaining and/or restoring the ecological status of natural water bodies, while also stressing the need to improve the ecological potential of heavily modified water bodies (HMWBs). This is to be achieved through the implementation of River Basin Management Plans (RBMPs), which involve the monitoring of hydrological, chemical, and biological indicators, as well as the application of appropriate restoration and mitigation measures (*Directive 2000/60/EC* 2000).

In Sweden 2.9% of the total water bodies are designated as heavily modified (HM) by hydropower and spatially, they are mostly located in the northern parts of the country comprising most of the large rivers. Yet only ten HMWBs are in good ecological potential class (1.5% of all HMWBs), and therefore, 98.5% of HMWBs are in less than good ecological potential as follows: 17 in moderate, 623 in poor and 18 in bad ecological potential. According to Sweden's 3rd RBMPs (2022-2027) only a modest improvement of the status of the surface water bodies is expected by 2027 (COMMISSION STAFF WORKING DOCUMENT Third River Basin Management Plans 2025; WISE EIONET Spatial Datasets s.d.). Hence, given the critical role of dissolved oxygen in supporting the structure and functioning of freshwater ecosystems, it is a pivotal factor in achieving and restoring ecological potential in heavily modified water bodies.

This study aimed to produce new scientific knowledge on the status and key drivers of DO in regulated rivers, with a focus on central and northern Sweden thereby contributing to the improvement of ecological potential in accordance with the objectives of the Water Framework Directive. Furthermore, the study aimed to provide guidance for future monitoring and restoration programs. I investigate the temporal and spatial variation of DO at an hourly resolution in three regulated (Luleälven, Umeälven, Ljungan) and two non-regulated rivers (Vindelälven, Piteälven) located in central and northern Sweden. The study aims to address the following questions:

- Do dissolved oxygen levels differ between regulated and free-flowing rivers?
- What are the main variables explaining spatial and temporal variation in dissolved oxygen?

I hypothesize that dissolved oxygen concentrations will be lower in regulated rivers compared to free-flowing ones due to hydrological alterations. Furthermore, I expect that temperature will be the main driver of dissolved oxygen in both experimental groups, as well as location, water depth, and flow will be the main variables explaining the spatial and temporal variation in dissolved oxygen.

2. Methods

2.1 Study area and sample site

The study was conducted in the central and northern Sweden, within the international basin districts SE2_INT and SE1_INT (*Directive 2000/60/EC* 2000; *WISE EIONET Spatial Datasets* s.d.), both included in the boreal biogeographic region. Within SE2_INT two regulated rivers, Umeälven and Luleälven were selected, which flow respectively within their homonymous catchments (26764 km², 25250 km², respectively). In contrast, within the same basin district, two of the last Swedish free-flowing rivers, Vindelälven which flows within Umeälven catchment, and Piteälven within its homonymous catchment 12304 km² were selected. In addition, within SE2_INT, Ljungan river was selected, which is the main stem of Ljungan catchment (12848 km²) (Figure 2).

Selected Regulated and non-regulated (free flowing) rivers display morphological and hydrological differences, as regulated rivers experienced intensive human exploitation since the early 50s, throughout dredging, damming, water diversion, and flow regime alteration, which profoundly impacted rivers' dynamism, connectivity, hydrologic regime, thus overall freshwater functional diversity. On the other hand, Free-flowing rivers display snowmelt hydrologic regimes that naturally occur in the boreal biographic region, maintaining most of their natural dynamics. (Poff & Ward 1990; Dynesius & Nilsson 1994; Poff et al. 1997; Nilsson et al. 2005; Poff & Zimmerman 2010; Parasiewicz et al. 2023). However, channel dredging for timber floating purposes partially altered morphology of free-flowing rivers. Overall, due to these morphological and hydrological differences, sample sites were chosen within each river to account for flow conditions and variables associated with it - either affecting it or affected by it - e.g. water mixing and retention time, zero flow events and depth. Sample sites in both groups were slow-flowing reaches with no silty bottom and the absence of visible macrophytes. The presence of silt and macrophytes reflect very slow-flowing reaches of backwater, in addition, macrophytes could bias DO daily cycle due to photosynthesis and respiration. Thus, to control for different conditions and further explore the site effect, each location was labelled as River, Lake, Reservoir, and Outlet, according to flow (figure 1), depth (figure 18) and morphological features.

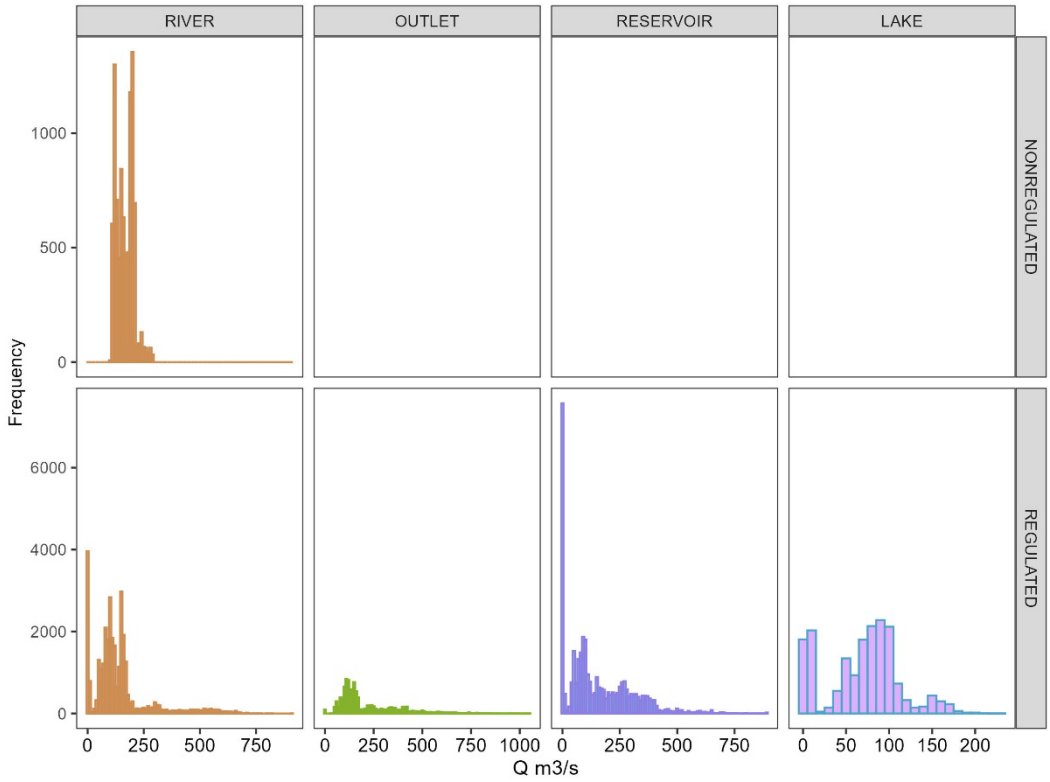

Figure 1: Frequency distribution of Total discharge [m^3/s] values for sites across different regulation classes. Each histogram represents the flow condition occurring within each specific site during the study period June-October 2024.

Once on the sample site, I collected site variables such as the Presence/absence of visible deadwood, the type of deadwood (log, debris, jam), the Percentage of boulders, cobble, pebble, granule, sand, and silt according to (Wentworth 1922), and the Decomposition (coverage %). Furthermore, the GPS location was collected via RTK station (REACH RS2+, by emlid) in SWEREF99 coordinates reference system (CRS). Right after, a stand-up paddleboard equipped with a portable sonar (STRIKER GPS by Garmin) was employed to scan the local bathymetry and estimate the approximate depth of the riverbed. The bathymetry map was created moving crosswise from the shore toward the centre of the channel several times to improve map resolution and accuracy. Thus, the map was recorded using the "*Garmin STRIKERcast*" app (Version: 1.5.794), to better identify the correct location and maintain track of the deployment depth. In total, 40 suitable sampling sites were identified where 49 Dissolved oxygen loggers were deployed as shown in the Figure 2.

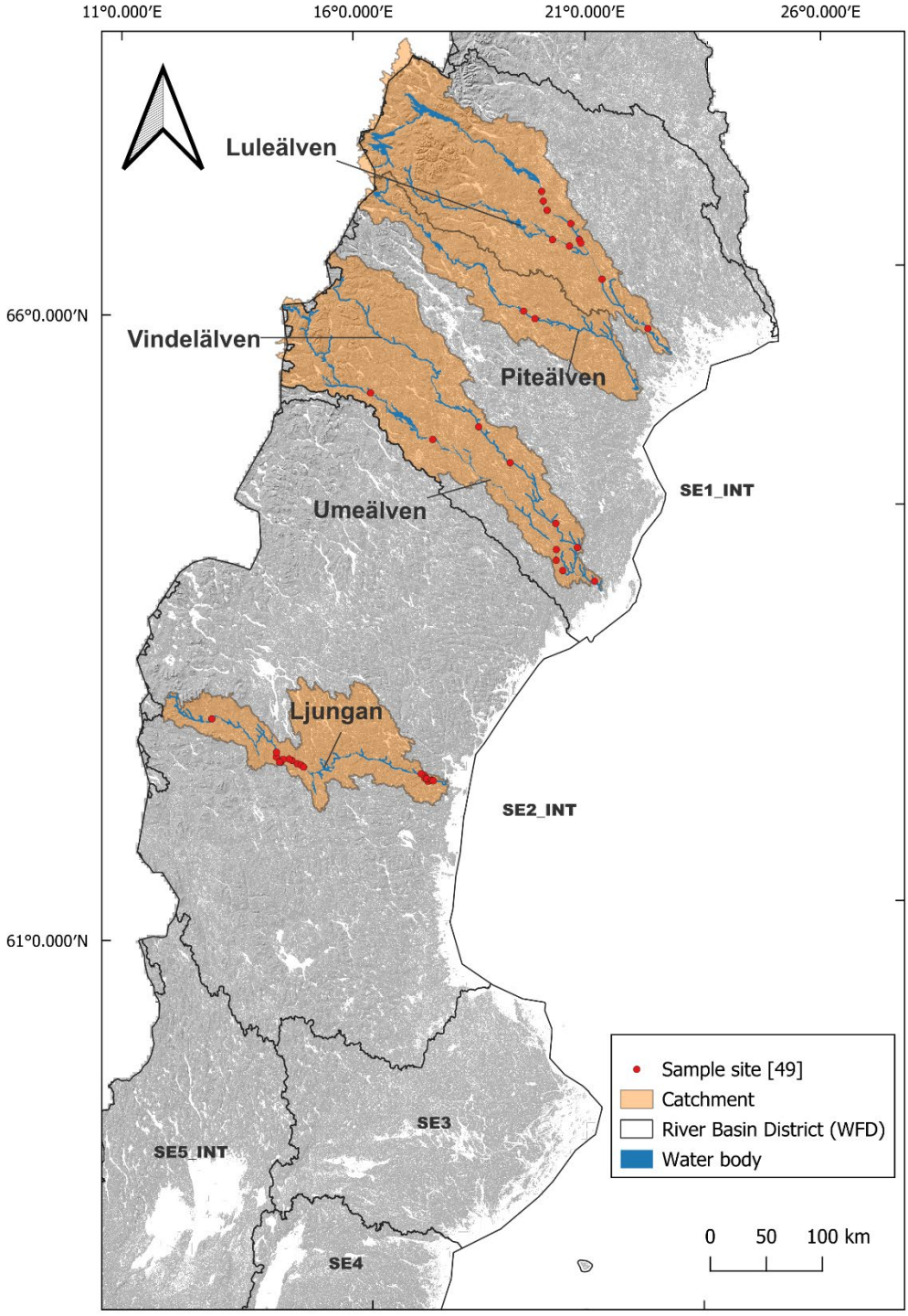

*Figure 2: The map shows sampling locations (red) where oxygen loggers were placed. Hydrography and River Basin District (RBD) designated by the Water Framework Directive were extracted from (*WISE EIONET Spatial Datasets *s.d.). Detailed map and information about sampling locations and waterbodies are available in the Appendix.*

2.2 Dissolved Oxygen loggers

The loggers used in this study were HOBO MX801[1] and HOBO U26-001[2] (by ONSET), optical dissolved oxygen (ODO) loggers with additional temperature sensors. The optic sensor operates using fluorescence quenching, a methodology that enable to estimate the density of dissolved oxygen based on the decrease in fluorescence intensity of a sample (water in front of the sensor during reading). Molecular oxygen is one of the best-known collisional quenchers (Lakowicz 2006). The optic sensors came with a factory calibration, however, according to the user manual to maintain accuracy below 4mg/l a "zero-point calibration" was needed before deployment. I calibrated the loggers to 0.05 mg/l using a sodium sulphite solution provided by the producer (ONSET, U26-CAL-SOL) following the recommended procedure in the user manual (*HOBO Dissolved Oxygen Logger (U26-001) Manual* s.d.; *MX800 Series User Guide | Onset's HOBO Data Loggers* s.d.). After calibration, the sensor was rinsed with running water to carefully remove the sodium sulphite residuals and stored with the provided boot, which contained a wet sponge, to keep the sensor moist until deployment. If not on logging mode, MX801 loggers automatically switched off a couple of minutes after Bluetooth disconnection.

The loggers were individually configured using "*HOBOconnect*" app (Version: 2.4.0) at 1-hour sampling interval for all loggers. After Bluetooth disconnection loggers automatically switched to battery saving mode, which means that loggers could automatically turn on every hour to collect and save the measurements, going back to "sleep mode" right after. Large logging capacity, sensor stability over time, and energy efficiency allow MX801 to potentially remain deployed for more than one year without maintenance. However, I experienced malfunctioning due to battery depletion in 5 deployed loggers, as probably, they did not autonomously switch to "sleep mode" causing complete discharge of the battery after approximately one and half months from the deployment. Deployment preceded by fastening loggers with several plastic ties to a brake disk to avoid transportation by the current, in addition, to enable later retrieving, the disk brakes were connected to a ø 3mm steel cable. The disk-logger system was then transported with the paddle board toward the channel centre, ensuring the location was as close as possible to the main flow, and at the chosen depth, thus, deployed.

To explore the effect of depth, I employed a hybrid experimental design, deploying 37 single loggers between 0 and 6m, and the remaining 12 loggers were deployed in transects, deploying loggers from shallow areas until the maximum

[1] Accuracy: Out-of-box: ±0.2 mg/L, typical over the range of 0 to 20 mg/L; ±4%, typical over the range of 20 to 60 mg/L With user calibration: ±0.1 mg/L over the range of 0 to 20 mg/L; ±2% over the range of 20 to 60 mg/L

[2] Accuracy: ±0.2 mg/L up to 8 mg/L; ±0.5 mg/L from 8 to 20 mg/L

depth available in the site within 100m from the shore, which was the maximum length of the metal cable reel. Each transect was composed by 4 loggers placed on regular depth intervals from 1.5 meters to the deepest available point. After deployment, the GPS location was acquired from each logger setting a waypoint on the sonar app, while the far end of the cable was fastened to a tree with a wire clamp. The same logger setting and deployment procedure was repeated for the 40 sample sites, resulting in the deployment of **49 loggers**. A total of 27 loggers were placed in Ljungan, (9 rivers, 12 lakes, 4 reservoirs, 2 outlets), 6 loggers in Umeälven (2 rivers, 1 lake, 3 reservoirs), 4 were placed in Umeälven (4 rivers), 2 in Piteälven (2 river), and 10 in Luleälven (1 river, 7 reservoirs, 2 outlet) (figure 17). The bulk of the loggers were placed in Ljungan to achieve other goals for projects outside this study.

2.3 Data collection and sources

Loggers were deployed on 2024-06-19 at 18:08:50 and remained submerged during summer from the middle of June 2024 until the beginning of October 2024. To retrieve them, we employed the same stand-up paddleboard-sonar framework, adding a 40 m steel cable ø 3mm, connected with a carabiner. The function of this cable was to connect with the carabiner the submerged metal guide, then follow the line until the logger position and lift the logger on the paddleboard. Concerning MX8001, loggers were lifted and turned to "wake" mode using the magnetic switch until the red LED control light blinked, signalling the logger was on and the Bluetooth was visible. Thus, using the "*HOBOconnect*" app, the data were downloaded as a xlsx file, and automatically saved in the app account for future export. While, for U26-001 loggers, which lack of Bluetooth connection, the data were exported as a csv file in the office, using a USB connection (all the specifics regarding data export are available on the MX8001 and U26-001 user manual (*HOBO Dissolved Oxygen Logger (U26-001) Manual* s.d.; *MX800 Series User Guide | Onset's HOBO Data Loggers* s.d.). Data were later gathered and stored in a 1TB external hard drive.

As mentioned in the previous section 5 MX801 loggers (LJTbD1, LJP009, LJTcD4, LJP020, VIP004) displayed empty batteries during data collection, therefore, batteries were inevitably replaced to download the data. The employed loggers have emergency saving mode, which triggers an emergency saving procedure in case of low power or malfunctioning, automatically saving the data history before turning off. During data collection, 3 loggers (LUP003, LJP014, VIP001) were found outside the water, as well as logger PIP002 was missing. Most of the loggers were retrieved before 2024-10-18, except for UMP005 and UMP006 which remained deployed until 21-11-2024.

I successfully exported data from 48 loggers out of 49, placing a total of 38 in the same position to collect data throughout the winter.

2.4 Data Processing and Cleaning

2.4.1 Sampling locations

Waypoints were exported from the Garmin app as a gpx file, Containing coordinates of 49 loggers in WGS84 CRS. This file was uploaded to QGIS (Maidenhead, version: 3.36), where coordinates were extracted. Similarly, shore points were exported from the RTK station as 5 separate files, uploaded in QGIS, and merged into a single point shapefile using the "*merge vector layers"* tool, selecting WGS84 as the destination CRS to homogenize layers. The field protocol was digitised in an Excel table with GPS locations and site information, including "River," "Logger ID," unique serial numbers, and deployment dates. Each logger was linked to the upstream powerplant, except LUP001, which was linked to the downstream one. This logger was 1,353 m from a reservoir dam (Porjus) at the head of Luleälven, where operations differ from other stations in the study (figure 35). Due to the lack of an upstream hydropower plant, the downstream one was assumed to drive flow conditions.

Additional spatial components, "Distance from the powerplant" and "Distance from the shore," were included. Distance from the powerplant was calculated in QGIS by drawing the shortest line from the logger to the plant along the river channel and computing length using the *length()* function. Distance from the shore was calculated in R({R Core Team} 2024) using the *st_nearest_feature()* function, available from the sf package (Pebesma & Bivand 2023) with logger and RTK locations as arguments. The final dataset included 23 columns and 48 rows.

2.4.2 Flow data

I received six months (2024-05-01 till 2024-10-31) of flow-operational data at 1-hour resolution from three Hydropower companies. These data are classified under the Trade Secrets Act (2018:558) as company secrets, and their usage is restricted. The provided datasets contained the unique name of each hydropower Plant station, related to two classes of operational data "Outlet flow [m^3/s]" and "Spill flow [m^3/s]", additionally the dataset contains the "Water level [MASL]" of the reservoir upstream the relative dam. In the provided datasets Outlet flow refers to the water flowing into the intake, reaching the turbine throughout the penstock, thus flowing out into the outlet channel. At the intake, a gate regulates the inflow, which is designed to avoid cavitation within the penstock, therefore its depth differs in each reservoir and depends on structural design. On the contrary, Spill flow refers

to the water flow regulated by a Tainter gate, which is a radial arm floodgate that controls water flowing into the spillway, that is often embodied by the old riverbed and is also known as bypass channel. Alternatively, the spill way can be an artificial concrete channel.

Data were from 21 plants: 7 in Ljungan, 8 in Luleälven, and 6 in Umeälven (tables 9, 12, 13). For free-flowing rivers, SMHI provided 11 years (2014–2024) of 1h flow data from stations 2237, 2238, 1630 (Vindelälven) and 1387 (Piteälven); 2024 data were used (tables 10, 11). Due to formatting inconsistencies, data were copied into 25 separate datasets (one per hydropower plant or SMHI station) with 6 columns each. For comparability, the same discharge was pasted in both "Outlet" and "Spill" columns in the non-regulated datasets. The hydropower plant column in these datasets was filled with the SMHI station name.

All datasets were uploaded in R, where timestamps were converted to date-time objects. "Outlet flow" values were corrected using minimum turbine capacity (Qmin) to compute the actual flow. Qmin values were provided for 8 stations (3 in Ljungan, 5 in Umeälven); for the remaining 13, a default Qmin of 20 m^3/s was used. For non-regulated rivers, Qmin was set to 1 m^3/s. "Real Outlet" was computed by replacing any "Outlet flow" values below Qmin with 0, then renamed as "Outlet."

A new variable, "Total flow," was calculated as the sum of "Spill flow" and "Outlet flow," representing downstream discharge. Another variable, "Zero flow," was added to identify absence of flow (TRUE if Total flow = 0; else FALSE). Then, a column "Total zero flow" was calculated as the cumulative number of consecutive hours with zero flow. All datasets (now 9 columns) were merged using *rbind()* into a single "Flow" dataset with 109,893 rows. Missing values were checked, and "Water level" was removed due to its absence in non-regulated rivers, resulting in a cleaned dataset with 8 columns and 109,893 rows, which was exported as a CSV file

.

2.4.3 DO Loggers data

Initially, 6 CSV files from U26-001 loggers were converted to XLSX format for data type consistency. All 48 logger files were then uploaded into R using *read_excel()* from the tidyverse R package (Wickham et al. 2019). Column names were standardized, and three new columns - "logger ID," "River," and "regulation class" (regulated/non-regulated)- were added for data integration. These 48 datasets were merged with *rbind()* into a single "all loggers" dataset with 6 columns and 130,448 observations. Variable classes were checked and adjusted: date-time was set to POSIXct format, while DO and temperature were set as numeric. Logging intervals were reviewed, identifying logger LJP015 with a 5-hour interval. As this discrepancy came from incorrect settings and did not affect zero-flow calculations, the data were retained. Logger activity periods were visualized using *geom_line()* from the ggplot2 R package (Wickham et al. 2019) (figure 23)

After, the loggers we found standing on the shore or discharged during data collection underwent visual inspection of raw temperature and DO data (figure 22). Among 8 problematic loggers (LJTbD1, LJP009, LJP020, LJP014, LJTcD4, VIP001, LUP003, VIP004), three (LUP003, LJP014, VIP001) with corrupted data were removed. The remaining five, despite battery issues, had reliable data and were retained. This cleaning step removed 5,221 observations, reducing the dataset to 125,227 entries.

Seven additional variables were then added applying *left_join()* from the dplyr package using logger ID as the key: "Depth [m]," "Distance from the shore [m]," "longitude," "latitude," "Site," "Powerplant ID," and "Distance of the Hydropower plant upstream [m]." To improve comparability, loggers were grouped into four depth classes: "0–3m," "3–6m," "6–9m," and ">9m." Distribution remained uneven, with 24 loggers in 0–3m, 14 in 3–6m, 3 in 6–9m, and 4 in >9m.

Non-regulated rivers had 5 loggers, all in 0–3m (4 in Vindelälven, 1 in Piteälven). In regulated rivers: 19 were in 0–3m, 14 in 3–6m, 3 in 6–9m, and 4 in >9m. Depth class distribution varied across rivers (figure 17): Ljungan had 10 (0–3m), 9 (3–6m), 3 (6–9m), and 4 (>9m); Luleälven had 4 (0–3m) and 5 (3–6m); Umeälven had 5 loggers, all in 0–3m.

Finally, the dataset was checked for missing values, and 28 failed DO and temperature entries were removed, resulting in a cleaned dataset with 45 loggers, 14 columns, and 125,199 observations.

Merging datasets

The "Flow" and "all loggers" datasets were merged to create a new dataset containing all necessary information to assess the effect of flow regulation on

Dissolved Oxygen at an hourly resolution. To ensure alignment, the date-time format of the logger dataset was adjusted using *as.POSIXct ()* function to remove minutes and seconds, converting timestamps to "Y-m-d & H" format (rounded to the hour). An additional variable, "ToD" (Time of Day), was added by extracting the hour of each measurement, resulting in cyclic values from 0 to 23. The final merged dataset included 121,188 rows and 20 columns and was exported as a CSV file. Further details on data cleaning and merging are provided in the Appendix (Supplementary methods).

2.5 Exploratory analysis

After cleaning and thinning, the final dataset was explored through descriptive statistics—percentage and total number of observations, minimum, maximum, mean, median, standard deviation, coefficient of variation, skewness, and kurtosis—for Dissolved Oxygen (Table 1) and Temperature (Table 4) across regulation classes. In parallel, descriptive statistics for Spill, Outlet, Total Flow (Table 5), and Zero Flow (Table 6) were computed by river.

The percentage of Dissolved Oxygen (DO) measurements within and outside the natural DO range for free-flowing rivers was quantified. The proportion of measurements falling below critical thresholds—DO < 5 mg/L (moderate hypoxia), DO < 3 mg/L (severe hypoxia), and DO = 0 mg/L (anoxia)—was calculated by regulation class. These thresholds were based on literature (Pollock et al. 2007; Diaz & Rosenberg 2008; Ekau et al. 2010; Davie 2019a; Fusi et al. 2023), reflecting minimum requirements for native lotic species (*Salmo salar, Salmo trutta, Thymallus thymmalus*), and macroinvertebrates like EPT taxa and the endangered *Margaritifera margaritifera*. While tolerance varies by species and life stage, thresholds were used as general indicators of potential ecological impact, rather than definitive limits.

Sampling effort (number of observations) was calculated by Regulation Class, River, Depth Class, Site, Distance from Hydropower Plant, and Distance from Shore, then visualized using *geom_bar()* and *geom_histogram()* from ggplot2 (Figures 15–19). DO distributions were visualized using *geom_violin()*, overlaid with *geom_boxplot()* by Regulation Class, River, and ID (Figures 3, 29, 32). The same structure was used to explore DO at increasing spatial resolution, from regulation class to river to individual logger ID. Temporal variation in DO was assessed using *geom_smooth()* with the GAM method from ggplot2, plotted at Regulation Class, River, and ID levels (Figures 3, 5, 30). Flow data were also explored using boxplots for Outlet, Spill, and Total Flow by River and Hydropower Station (Figures 32–34). Temperature and Total Zero Flow were visualized through

boxplots. To examine the Temperature–DO relationship, a scatterplot was created using *geom_point()*, grouped by Regulation Class (Figure 35), and another showed DO over time coloured by River (Figure 36). DO distributions during Zero Flow events were visualized with a violin plot (Figure 27). Violin plot combined with boxplot allows to display the shape of the data distribution combined with its statistics (quartile, maximum, minimum, outliers).

Lastly, an 11x11 correlation matrix was calculated using *cor()* from the corrplot package (Taiyun Wei & Viliam Simko 2024), applying Spearman's method to accommodate non-normality. The matrix was plotted separately for each Regulation Class to highlight differences in predictor relationships (Figure 20).

2.6 Modelling

Data exploration revealed high variability in Dissolved Oxygen (DO) measurements, both within and between different IDs, particularly in non-regulated rivers. This variability emphasized the need for a flexible and robust regression approach. To avoid assuming a fixed functional form and to handle heavy-tailed distributions, we applied Generalized Additive Models (GAMs). GAMs are likelihood-based regression models that are less reliant on the assumption of normality and are well-suited for capturing non-linear relationships by estimating the functional form directly from the data.

GAMs express the response variable as the sum of smooth functions of each predictor, following the general formula:

$$\boldsymbol{y_i = \beta_0 + \sum_j s_j(x_{ji}) + \in_i}$$

Equation 1: GAM general equation

Where $\boldsymbol{s_j}$ are smooth functions (splines) fitted to the data (Pedersen et al. 2019).

In this study, we used the *bam ()* function from the mgcv R package (Wood 2017) to model DO. bam () is optimized for large datasets through the fast Restricted Maximum Likelihood (fREML) algorithm and a discrete approximation method, reducing computational cost. It also supports various distribution families; given the heavy-tailed nature of our data, we specified a scaled-t distribution using family = scat (), which offers greater robustness than the Gaussian.

Temporal patterns were addressed by including *Date* as a numerical smooth term to capture autocorrelation. *ID* and *River* were included as random effects to model

site-related variability not explained by predictors. We first built a univariate model with *Regulation class* as a fixed effect to test for differences in DO between regulated and non-regulated rivers (reference category: “non-regulated”). Model selection followed, based on iterative addition/removal of variables identified via the correlation matrix, resulting in 20 multivariate models ranked by AIC. Model *MM19*, with the lowest AIC, was selected for diagnostics using *gam.check()* Diagnostic plots revealed slight under-fitting in the smooth terms for Outlet flow, Spill flow, and Date. To improve flexibility, the basis dimension parameter (k) for these predictors was increased from 20 to 30, which notably improved model fit. This refined model, with optimized smoothness, was retained as the final multivariate model (MM).

3. Results

3.1 Dissolved oxygen summary statistics

Exploring summary statistics of dissolved oxygen (DO) measurements revealed differences between regulated and non-regulated rivers. Although the mean DO concentration was similar across the two groups, 9.7 mg/l ± 0.008 in non-regulated, and 9.4 mg/l ± 0.004 In regulated rivers, the distribution of measurements differed significantly. Data in regulated rivers showed a heavy-tailed distribution with strong left skewness (Skewness = -2.9) and high kurtosis (Kurtosis = 22.0). In contrast, the non-regulated rivers had a more symmetrical distribution (Skewness = 1.0; Kurtosis = 5.0). Furthermore, the minimum DO value was much lower in regulated rivers (0.0 mg/l) compared to non-regulated ones (7.4 mg/l). In terms of variability, regulated rivers also showed higher standard deviation (S.D.=1.2) and coefficient of variation (C.V. = 12.8) than non-regulated rivers (S.D. = 0.7; C.V. = 7.2), stressing the presence of greater fluctuations in DO levels.

Table 1: Descriptive statistics of dissolved oxygen (DO) concentration across regulation classes. Minimum (Min), maximum (Max), standard error (S.E.), standard deviation (S.D.), coefficient of variation (C.V.), median, skewness, and kurtosis of dissolved oxygen concentrations [mg/l] relative to the study period June-October 2024 in Sweden

D.O. Parameters	**NONREGULATED (N=9295)**	REGULATED (N=97153)
Obs. %	**8.7**	91.3
Min [mg/l]	**7.4**	0.0
Max [mg/l]	**12.6**	14.3
Mean [mg/l]	**9.7**	9.4
S.E.	**0.008**	0.004
S.D.	**0.7**	1.2
C.V.	**7.2**	12.8
Median [mg/l]	**9.6**	9.4
skewnes	**1.0**	-2.9
kurtosis	**5.0**	22.0

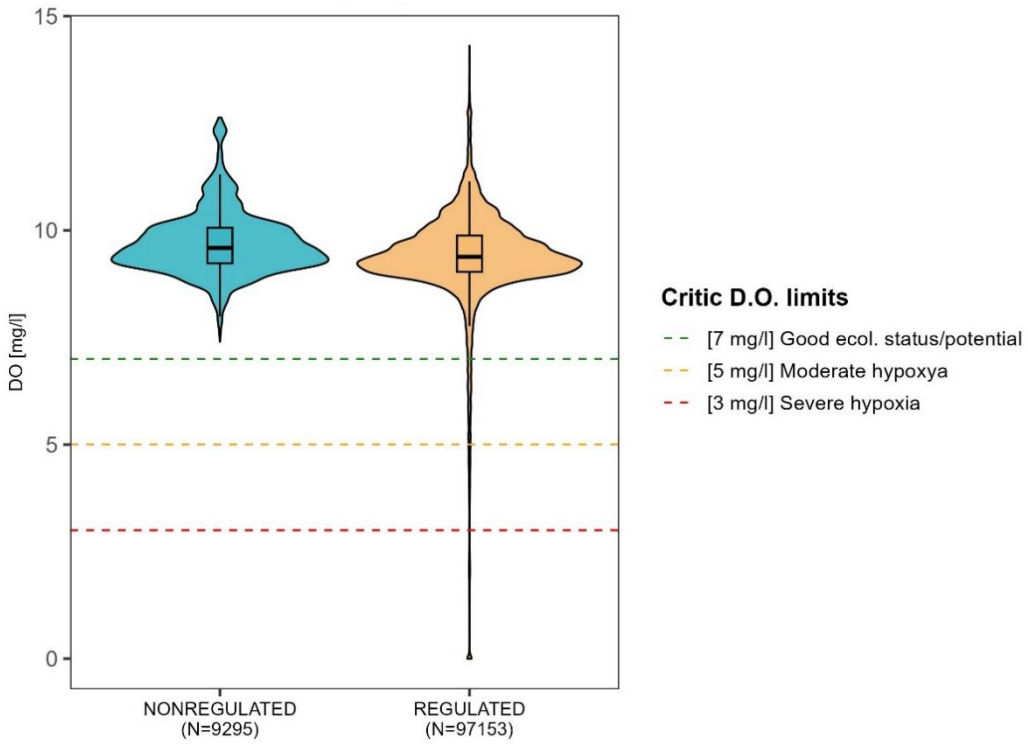

Figure 3: Distribution of dissolved oxygen (DO) across regulation classes. Violin plots show the distribution of DO measurements [mg/l] in regulated and non-regulated rivers. The inner boxplots represent the median interquartile range (IQR), and whiskers (showing minim and maximum without outliers). Horizontal reference lines indicate ecologically relevant thresholds: 7mg/l (minimum for good ecological status), 5 mg/l (moderate hypoxia), and 3 mg/l (severe hypoxia). Data are relative to the study period June-October 2024 in Sweden.

Extreme low values and the related heavy tailed distribution was detectable at river resolution with regulated rivers (Ljungan, Luleälven, Umeälven) displaying hypoxic and even anoxic DO levels (1.0 mg/l, 0.0 mg/l, 3.3 mg/l respectively). Again, non-regulated rivers Piteälven and Vindelälven showed relatively higher minimum levels (7.4 and 8.2 mg/l) and low variability

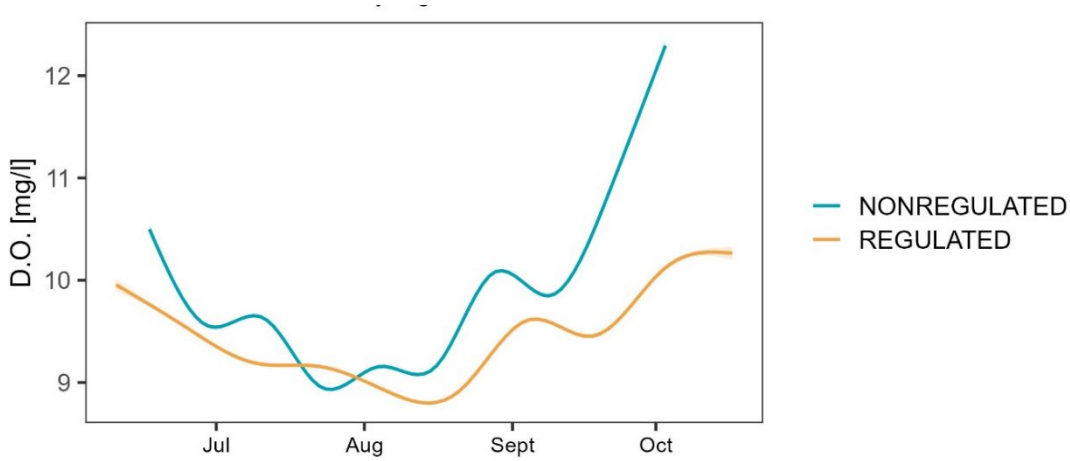

Figure 4: Temporal variation in dissolved oxygen (DO) concentration across regulation classes. Smoothed trend lines (GAMs) show changes in dissolved oxygen concentration in mg/l over the study period (June-October 2024) for regulated and non-regulated rivers in Sweden. Shaded areas represent 95% confidence intervals.

Table 2: Descriptive statistics of dissolved oxygen (DO) concentration across river. Minimum (Min), maximum (Max), mean, standard error (S.E.), standard deviation (S.D.), coefficient of variation (C.V.), median, skewness, and kurtosis of dissolved relative to the study period June-October 2024 in Sweden.

D.O. Parameters	LJUNGAN (N=57334)	LULEA (N=22664)	**PITEA (N=2577)**	UMEA (N=17155)	**VINDELN (N=6718)**
Obs. %	53.9	21.3	**2.4**	16.1	**6.3**
Min [mg/l]	1.0	0.0	**7.4**	3.3	**8.2**
Max [mg/l]	11.8	13.6	**12.6**	14.3	**12.5**
Mean [mg/l]	9.4	9.4	**9.8**	9.4	**9.7**
S.E.	0.003	0.011	**0.018**	0.012	**0.008**
S.D.	0.7	1.6	**0.9**	1.6	**0.7**
C.V.	7.5	17.3	**9.1**	16.6	**6.8**
Median [mg/l]	9.3	9.5	**9.8**	9.6	**9.5**
skewness	-2.2	-3.5	**0.5**	-0.9	**1.2**
kurtosis	20.6	19.6	**4.0**	4.6	**5.4**

Extreme low values and the related heavy tailed distribution was detectable at river resolution with regulated rivers (Ljunganälven, Luleälven, Umeälven) displaying hypoxic and even anoxic DO levels (respectively 1.0 mg/l, 0.0 mg/l, 3.3 mg/l).

Again, non-regulated rivers Piteälven and Vindelälven showed relatively higher minimum levels (7.4 and 8.2 mg/l) and low variability (C. V= 9.1 and 6.8)

A more in-depth exploration of Dissolved Oxygen (DO) revealed that 96.9% of the measurements in regulated rivers fell within the optimal range for freshwater lotic ecosystems (7–13 mg/L). In comparison, 100% of the measurements in non-regulated rivers remained above 7mg/l.

Table 3: Proportion of dissolved oxygen (DO) observations within ecologically relevant thresholds across regulation classes (Pollock et al. 2007; Diaz & Rosenberg 2008; Davie 2019a; Fusi et al. 2023). Percentage of observations (%) falling into five DO classes across regulated and non-regulated rivers in Sweden during the study period June-October 2024: >13mg/l (supersaturation), 7-13 mg/l (good ecological status), <7 (minimum of good status), <5 mg/l (moderate hypoxia), and <3 (severe hypoxia).

D.O. Parameters	**NONREGULATED (N=9295)**	REGULATED (N=97153)
DO>13 mg/l [%]	**0**	0.1
7 ≥ DO ≤ 13 mg/l [%]	**100**	96.9
DO<7 mg/l [%]	**0**	2.9
DO<5 mg/l [%]	**0**	1.2
DO<3 mg/l [%]	**0**	0.8
DO= 0 mg/l [%]	**0**	0.2

Furthermore, in regulated rivers, 2.9% of DO values were below 7 mg/L, 1.2% of the measurements fall below the range of moderate hypoxia (DO < 5 mg/L), 0.8% severe hypoxia (DO < 3 mg/L), and 0.2% anoxic conditions (DO = 0 mg/L). These critical low values were not observed in non-regulated rivers.

Results of univariate GAM (UM.REG), which compared DO concentration between regulated and non-regulated rivers show that the regulated rivers showed a statistically significant lower levels of DO, i.e. −0.183 mg/L (S. E. = 0.007352; t-value = −24.9; P<0.001; n = 106,448)

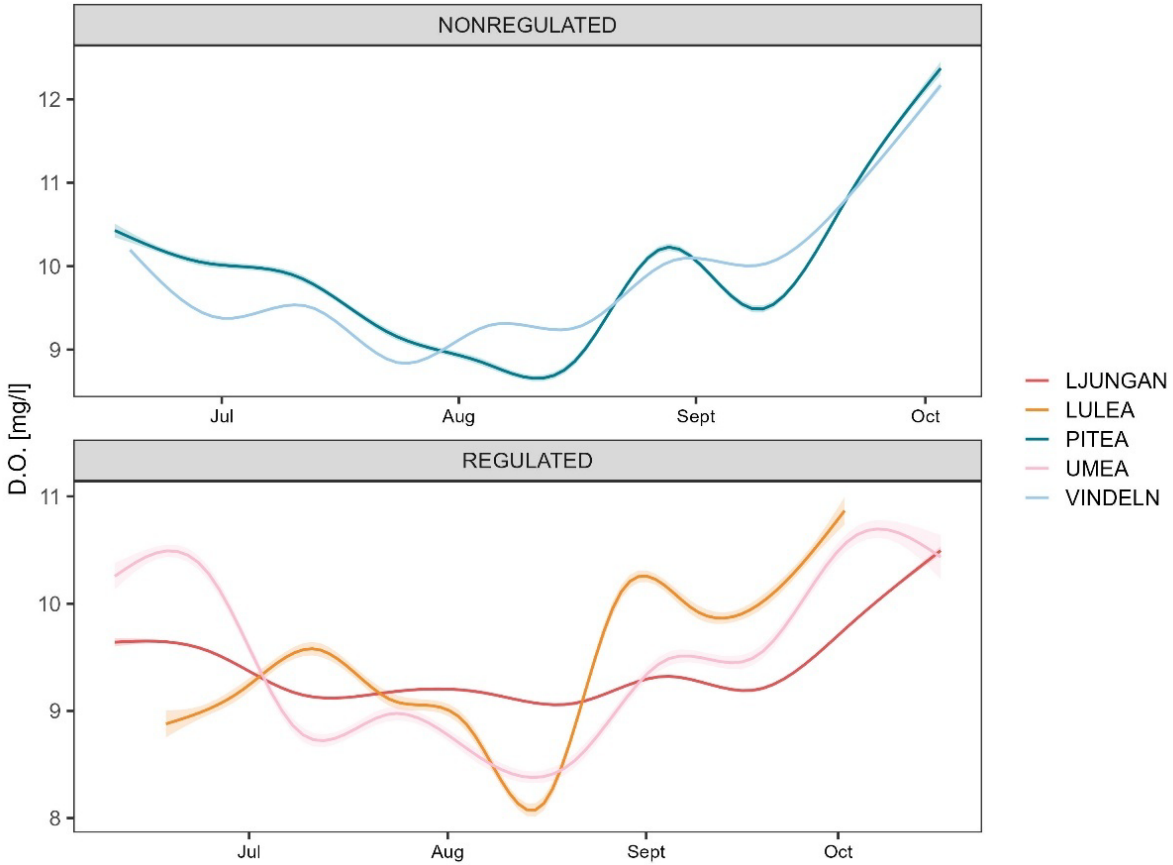

Figure 5: Temporal variation in dissolved oxygen (DO) concentration across selected rivers in Sweden. Smoothed trend lines (GAMs) show changes in dissolved oxygen concentration [mg/l] over the study period June-October. Shaded areas represent 95% confidence interval

3.2 Predictors summary statistics

3.2.1 Temperature

The exploration of temperature values did not show strong differences in the overall data distribution between regulated and non-regulated rivers. Both groups had similar ranges and central tendencies, with non-regulated rivers showing a slightly higher mean (16.1 °C ± 0.033) compared to regulated ones (15.8 °C, ±0.01). Measures of spread and shape, including standard deviation (non-reg S.D=3.1, reg S.D=3.0), coefficient of variation (non-reg C. V=19.3, reg CV=19.0), skewness, and kurtosis, were also very similar (Table 4) across the two classes.

While both dissolved oxygen and temperature showed statistically significant differences between regulated and non-regulated rivers, the patterns of variation were not equally pronounced. DO levels showed clear distributional differences, including more extreme low values and greater variability in regulated rivers. In contrast, temperature differences were more subtle. Although the GAM model detected a small but significant decrease in temperature in regulated rivers, the overall distribution of temperature values remained similar across both regulation classes.

Table 4: Descriptive statistics of water temperature across regulation classes. Minimum (Min), maximum (Max), mean, standard error (S.E.), standard deviation (S.D.), coefficient of variation (C.V.), median, skewness, and kurtosis of water temperature [°C] relative to the study period June-October 2024 in Sweden.

Variable	**NONREGULATED (N=9295)**	REGULATED (N=97153)
Obs. %	**8.7**	91.3
Min [°C]	**4.7**	0.0
Max [°C]	**22.0**	21.6
Mean [°C]	**16.1**	15.8
S.E.	**0.033**	0.01
S.D.	**3.1**	3.0
C.V.	**19.3**	19.0
Median [°C]	**16.7**	16.4
skewnes	**-1.2**	-1.0
kurtosis	**4.6**	3.7

3.2.2 Flow (Outlet, Spill, Total)

The summary statistics of outlet, spill, and total flow were calculated by river, showing that zero flow (Total flow = 0) occurred in all the regulated rivers while this condition resulted to be absent in non-regulated rivers (table 5)

Regulated rivers also showed higher variation in all types of flow compared to the natural rivers, especially concerning spill flow, reflected by the higher standard deviation (S.D.) and coefficient of variation (C.V.) values. In contrast, the free-flowing rivers (Vindelälven and Piteälven) displayed lower variability, mirroring more stable flow during the study period.

Table 5: Descriptive statistics of Outlet, Spill and Total discharge [m^3/s] across selected rivers. Minimum (Min), maximum (Max), mean, standard error (S.E.), standard deviation (S.D.), coefficient of variation (C.V.), median, of water discharge [m^3/s] relative to the study period June-October 2024 in Sweden.

Variable	LJUNGAN (N=57334)	LULEA (N=22664)	**PITEA (N=2577)**	UMEA N=17155)	**VINDELN (N=6718)**
Outletflow[m^3/s]					
Min	0.0	0.	**149.4**	0.0	**104.8**
Max	229.0	883.0	**291.6**	908.0	**272.6**
Mean	80.6	181.4	**197.2**	202.3	**155.8**
S.E.	0.2	1.2	**0.5**	1.2	**0.4**
Median	83.3	171.0	**197.8**	194.0	**148.5**
S.D.	50.3	173.2	**26.1**	161.1	**36.1**
C.V.	0.6	1.0	**0.1**	0.8	**0.2**
Spillflow [m^3/s]					
Min	0.0	0.0	**149.4**	0.0	**104.8**
Max	174.0	1,005.0	**291.6**	443.0	**272.6**
Mean	7.4	36.0	**197.2**	23.1	**155.8**
S.E.	0.1	0.8	**0.5**	0.4	**0.4**
Median	0.0	0.0	**197.8**	0.0	**148.5**
S.D.	17.8	123.2	**26.1**	55.0	**36.1**
C.V.	2.4	3.4	**0.1**	2.4	**0.2**
Totalflow[m^3/s]					
Min	0.0	0.0	**149.4**	0.0	**104.8**
Max	229.7	1,047.0	**291.6**	908.0	**272.6**
Mean	88.1	217.4	**197.2**	225.4	**155.8**
S.E.	0.2	1.3	**0.5**	1.2	**0.4**
Median	89.5	202.0	**197.8**	222.1	**148.5**
S.D.	46.8	198.5	**26.1**	162.5	**36.1**
C.V.	0.5	0.9	**0.1**	0.7	**0.2**

3.2.3 Zero flow

Exploration of zero flow events showed clear differences between regulated and non-regulated rivers. Regulated rivers displayed occurrence of zero flow events, while zero flow was not detected in the non-regulated rivers. Among the regulated rivers, Luleälven and Umeälven experienced the longest zero flow durations (table 6), with events lasting up to 152 and 145 hours, respectively. The average duration of zero flow was also higher in Luleälven (6.9 hours, S.E.=0.12) and Umeälven (2.3 hours, S.E.=0.07), compared to Ljunganälven (0.3 hours, S.E.=0.01). The total number of days with zero flow was higher in Luleälven (32.6 days), followed by Umea (17.9 days) and Ljunganälven (6.6 days).

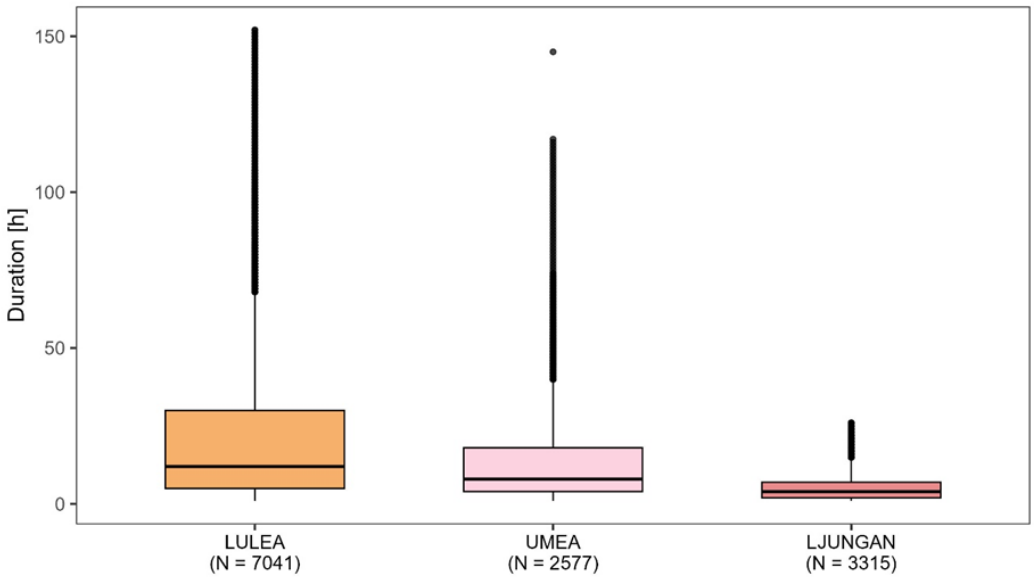

Figure 6: Boxplots of zero-flow event duration across regulated rivers. Boxplots show the distribution of durations [hours] of zero-flow events occurred during the study period June-October 2024 in selected regulated rivers in Sweden. Each box represents the median (black line inside the box), interquartile range (IQR), whiskers (showing minim and maximum without outliers), and extremes (which were not considered outliers). This chart highlights the frequency and variability in duration of flow interruption caused by hydropower operational schemes.

Table 6: Descriptive statistics of zero-flow across selected rivers. Total days of survey, minimum (Min), maximum (Max), mean, standard error (S.E.), standard deviation (S.D.), coefficient of variation (C.V.), median and cumulative time of zero-flow [day] relative to the selected rivers over the study period June-October

Variable	LJUNGAN (N=57334)	LULEA (N=22664)	**PITE (N=2577)**	UMEA (N=17155)	**VINDELN (N=6718)**
Survey[day]	129.0	106.0	**107**	129.0	**106**
Min [h]	0.0	0.0	**0**	0.0	**0**
Max [h]	26.0	152.0	**0**	145.0	**0**
Mean [h]	0.3	6.9	**0**	2.3	**0**
S.E.	0.01	0.12	**0**	0.07	**0**
Median [h]	0.0	0.0	**0**	0.0	**0**
S.D.	1.7	17.6	**0**	8.9	**0**
C.V.	5.4	2.6	**NA**	3.9	**NA**
Tot zero flow [day]	6.6	32.6	**0**	17.9	**0**

3.2.4 Depth

Dissolved oxygen data when grouped by depth class revealed greater fluctuations within the 0–3 m depth range (C.V. = 15.1). Additionally, DO concentrations were, on average, lower in this surface layer (9.3 mg/l, ±0.01) compared to the 3–6 m depth class (9.5 mg/l, ± 0.001) and the 6–9 m class (9.7 mg/l, ±0.01), which showed the highest average oxygen concentration. Furthermore, DO exhibited distinct temporal variation patterns across the different depth during summer.

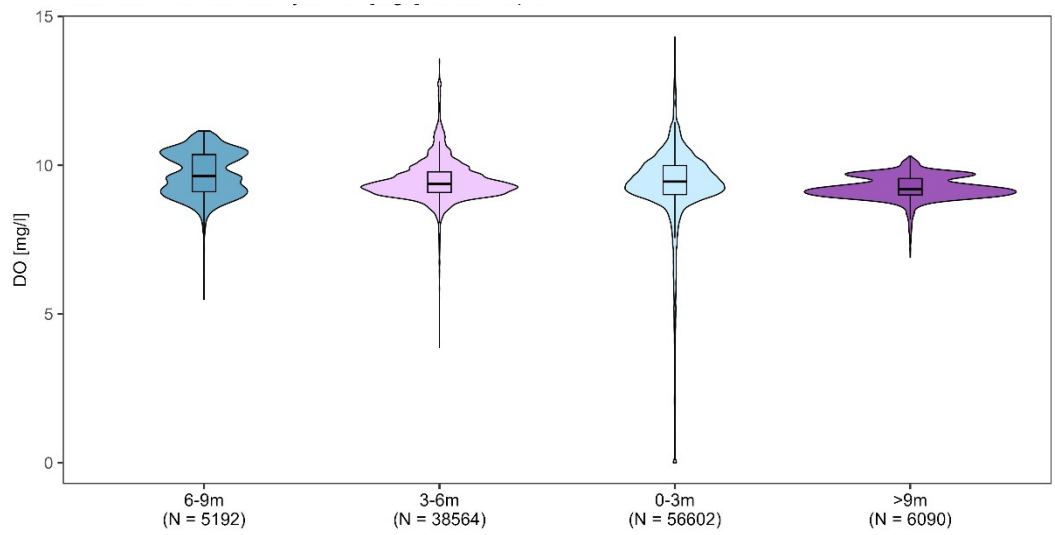

Figure 7: Distribution of dissolved oxygen (DO) across selected depth classes 0-3m, 3-6m, 6-9m and <9m. Violin plots are displayed in descending order of DO based on the median value, and show the distribution of DO measurements in mg/l. The inner boxplots represent the median, interquartile range (IQR), and whiskers (showing minim and maximum without outliers). Data are relative to the study period June-October 2024 in Sweden.

.

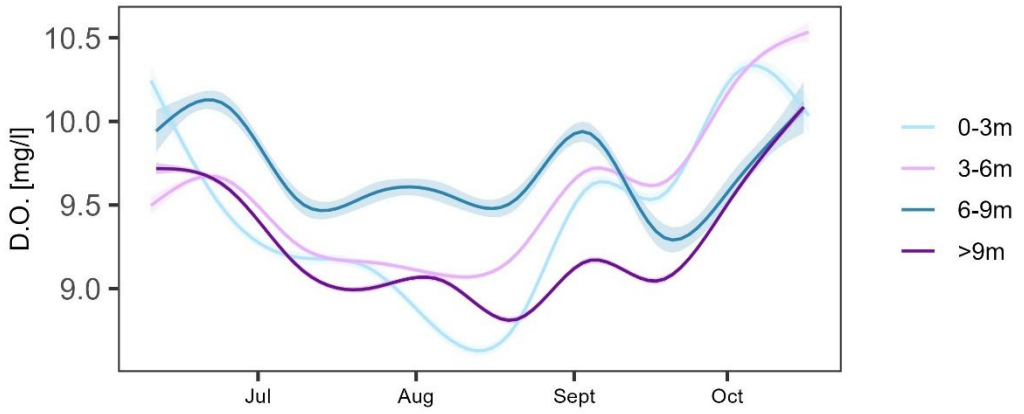

Figure 8: Temporal variation in dissolved oxygen (DO) concentration across selected depth classes 0-3m, 3-6m, 6-9m and <9m. Smoothed trend lines (GAMs) show changes in DO concentration in mg/l relative to each depth class over the study period June-October 2024 in Sweden. Shaded areas represent 95% confidence interval

3.2.5 Sampling site effects

Exploration of DO across sites and regulation classes revealed notable differences in the occurrence of extreme values. In regulated rivers, reservoirs and lakes, which also experience lower flow rates (figure 1) the data showed high frequency of extreme DO levels (Reservoir CV = 14.4; Lake CV = 10.5). These sites also recorded more extreme minimum values (Reservoir min = 0 mg/L, Lake min = 1 mg/L). Furthermore, river conditions exhibited moderate fluctuation in DO concentrations (CV = 12, min = 3.3 mg/L), with a distribution visually distinct from the non-regulated rivers, which had a lower coefficient of variation (CV = 7.6), and higher minimum DO concentrations (min = 7.4 mg/L).

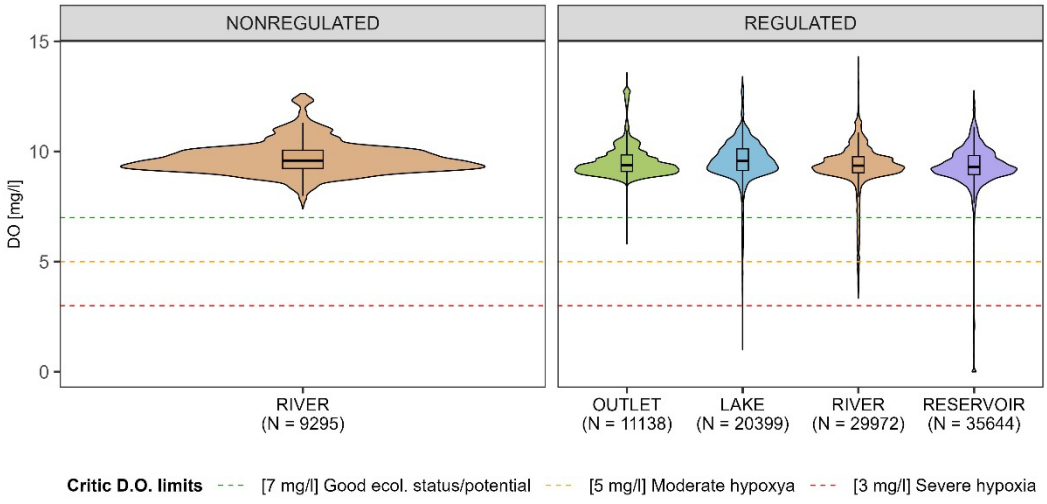

Figure 9: Distribution of dissolved oxygen (DO) across selected sites by regulation class. Violin plots show the distribution of DO measurements in mg/l relative to each site. The inner boxplots represent the median, interquartile range (IQR), and whiskers (showing minim and maximum without outliers). Horizontal reference lines indicate ecologically relevant thresholds: 7mg/l (minimum for good ecological status), 5 mg/l (moderate hypoxia), and 3 mg/l (severe hypoxia). Data are relative to the study period June-October 2024 in Sweden

3.3 Correlates affecting Dissolved oxygen

A total of 20 Generalized Additive Models (GAMs) were fitted and then compared using the Akaike Information Criterion (AIC) to explore the role of the different factors influencing dissolved oxygen levels. As expected, Temperature was the strongest initial predictor, however, model performance improved as more variables were added, especially those related to different types of flow (outlet, spill, total zero-flow), as well as time of day (ToD), and variation in time (DATE) played an important role. Including spatial effects (longitude, latitude), ID and river identity also helped explain more variability, However, longitude and latitude lost

significance quite early in the selection process, thus were not included in the final model (table 7).

The best-performing models were those with the lowest AIC values (109433.2 and 109433.4, respectively). These models used separate smoothers for outlet and spill flow and included temperature and date as individual smoother terms by regulation class, which gave a better fit than models which used total flow or a combined “temperature-date” interaction (tensor product smoother = te()). Models that replaced outlet/spill with total flow or used the tensor product smooth showed higher AIC, indicating a reduction in model performance.

The selected models explained about 53.9% of the DO deviance, with an adjusted R^2 of 0.38, showing a good overall fit. Temperature had a strong ($P<0.001$) and complex effect, especially in regulated rivers ($F = 3269.7$) (non reg. $F=41.428$) showing a strong non-linear response. Time of day (ToD) also significantly influenced DO in both river types ($P<0.001$), mirroring the natural DO cycle, nevertheless, a greater effect was detected in regulated systems ($F = 347.9$) (non reg $F=61.3$) (table 8). Including “River" as a random effect did not improve the model’s explanatory power or performance, and the effect was not statistically significant, while Outlet and spill flows resulted to be significant predictors only in regulated rivers, respectively ($P<0.001$, $F = 158.6$, and $P<0.001$, $F = 731.4$). Cumulative time of Zero-flow (tot.z.flow) was also significant ($P<0.001$, $F = 49.9$), showing that the absence of flow also played an important role in driving DO values. Moreover, the model highlights that during relatively short zero flow events dissolved oxygen tends to fluctuate while prolonged absence of flow leads to a steady decline. Time and thus Temporal autocorrelation were modelled through the smooth term of date, which resulted to be much more complex in regulated systems ($P<0.001$, $F = 1719.1$) compared to free-flowing rivers ($P<0.001$, $F = 75.4$) which showed a more stable trend.

Depth class had no significant effect, and including river identity as a random effect in ($F = 0.001$, $p = 0.27$), suggesting that ID as random effect and the weight of the other predictors already captured most of the differences between rivers. The model showed that separating flow components (outlet, spill) and modelling temperature and time independently by regulation class gives a more accurate understanding of the drivers of DO, further suggesting an effect of water regulation. The evaluation of the best-performing model with *check.gam ()* function, from mgcv R package(Wood 2017) confirmed a good overall fit, with achieved convergence. However, basis dimension (k) checking revealed that some smooth terms, particularly outlet flow, spill flow, and Date, were slightly underfitted, as indicated by low k-index values and significant p-values ($P<0.05$). To address this,

a refined model was developed by increasing the basis dimension (k) of Outlet flow, Spill flow, and Date from 20 to 30. These adjustments were intended to provide more flexibility in the smoothers and better capture the unmodelled variation in the data.

Optimization of the basis dimensions led to a substantial improvement in model performance, as showed by a reduction of approximately 500 AIC points (MM19: AIC = 109433.2; MM: AIC = 108922.3), although the proportion of deviance explained and the adjusted R^2 showed only marginal gains in the final model (Deviance explained = 54%; Adjusted R^2 = 0.38). The k-index marginally improved for Spill and Date, while slightly get worse for temperature and ToD. Notably, in the final model Spill flow term became highly significant for non-regulated rivers, however the wiggle of the smooth function clearly differs from the regulated one which displayed a higher degree of complexity (non-regulated EDF=9.29, regulated EDF=28.8) and a differed effect (non-regulated F=36.27, regulated F=500.97).

Table 7: Variables used for Multivariate model selection based on Akaike Information Criterion (AIC).Formula shows covariates included in each model, such as temperature, regulation class (REG), date, site ID, time of day (ToD), Outlet and Spill discharge, total flow (TOT), depth class, spatial coordinates (latitude, longitude), and river characteristics. MM is the updated version of MM19 improving k-index. Results from MM were used for this study (figure10).

Model	Formula	AIC
MM1	TEMPERATURE, REG	199,548.1
MM2	TEMPERATURE, REG, DATE	178,052.9
MM3	TEMPERATURE, REG, DATE, ID	127,186.9
MM4	TEMPERATURE, REG, DATE, ID, ToD	119,311.8
MM5	TEMPERATURE, REG, DATE, ID, ToD, OUTLET	116,309.3
MM6	TEMPERATURE, REG, DATE, ID, ToD, OUTLET, SPILL	111,543.4
MM7	TEMPERATURE, REG, DATE, ID, ToD, TOT	114,598.5
MM8	ID, ToD, REG, TOT, te(DATE, TEMPERATURE)	112,470.5
MM9	ID, ToD, REG, TOT, te(DATE, TEMPERATURE), TOT.Z. FLOW	112,294.1
MM10	ID, ToD, REG, TOT, te(DATE, TEMPERATURE), TOT.Z. FLOW, Z. FLOW	112,290.9
MM11	ID, ToD, REG, TOT te(DATE, TEMPERATURE), TOT.Z. FLOW, Z. FLOW, DEPTH.CLASS	112,286.9
MM12	ID, ToD, REG, TOT, te(DATE, TEMPERATURE), TOT.Z. FLOW, Z. FLOW, DEPTH.CLASS, DIST.SHORE	112,288.5
MM13	ID, ToD, REG, TOT, te(DATE, TEMPERATURE), TOT.Z. FLOW, Z. FLOW, DEPTH.CLASS, DIST.HP. UP	112,288.3
MM14	TEMPERATURE, REG, DATE, ID, ToD, OUTLET, SPILL, DEPTH.CLASS	111,543.7
MM15	TEMPERATURE, REG, DATE, ID, ToD, OUTLET, SPILL, DEPTH.CLASS, TOT.Z. FLOW	111,182.3
MM16	TEMPERATURE, REG, DATE, ID, ToD, OUTLET, SPILL, DEPTH.CLASS, TOT.Z. FLOW, LONGITUDE, LATITUDE	111,183.0
MM17	TEMPERATURE, REG, DATE, ID, ToD, OUTLET, SPILL, DEPTH.CLASS, Z. FLOW	111,314.6
MM18	TEMPERATURE, REG, DATE, ID, ToD, OUTLET, SPILL, DEPTH.CLASS, TOT.Z. FLOW, RIVER	111,182.4
MM19	**TEMPERATURE, REG, ID, ToD, OUTLET, SPILL, DEPTH.CLASS, TOT.Z. FLOW, DATE**	**109,433.2**
MM20	TEMPERATURE, REG, ID, ToD, OUTLET, SPILL, DEPTH.CLASS, TOT.Z. FLOW, DATE, RIVER	109,433.4
MM21	TEMPERATURE, REG, ID, ToD, OUTLET, SPILL, DEPTH.CLASS, TOT.Z. FLOW, DATE, SITE	109,433.4
MM	**TEMPERATURE, REG, ID, ToD, OUTLET k=30, SPILL k=30, DEPTH.CLASS, TOT.Z. FLOW, DATE k=30**	**108,922.3**

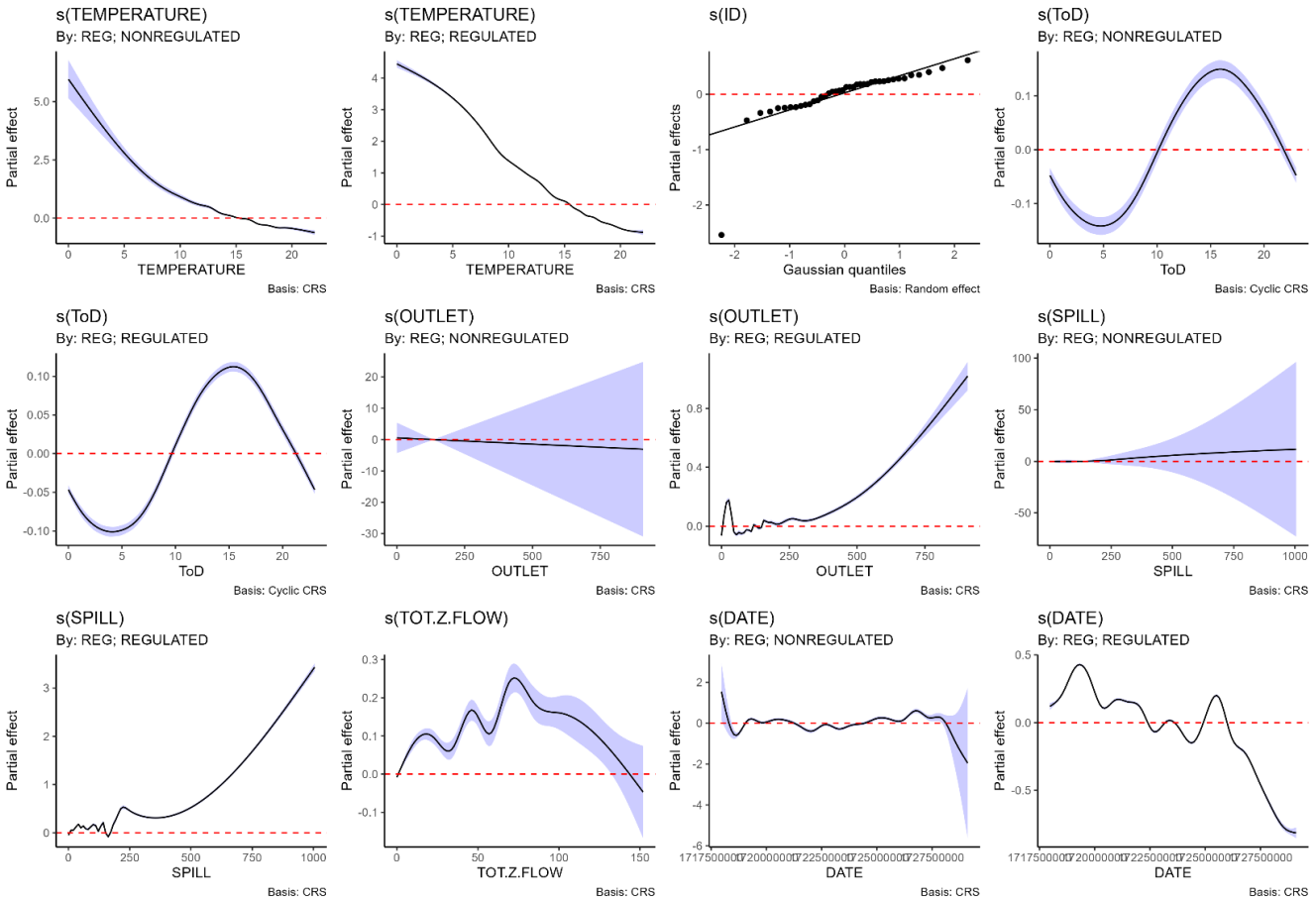

Figure 10: Partial effects of predictor variables on dissolved oxygen (DO) from the final model. Plots show the smooth terms from the final GAM (MM), illustrating the estimated non-linear relationships between predictors and DO concentration. Each predictor ***Temperature***, ***Date***, ***Time of Day (ToD)***, ***Outlet***, *and* ***Spill flow*** *is visualized separately for* ***regulated*** *and* ***non-regulated*** *rivers. The variable* ***ID****, included as a random smoother (i.e., random effect), displays deviations from the overall model intercept, accounting for spatial variability. The effect of* ***total zero-flow duration (TOT.Z.FLOW)*** *is shown only for regulated rivers, where such events occur. Shaded (blue) areas represent 95% confidence intervals. All effects are shown as partial residuals, with other model terms held constant, showing individual contribution of each variable.*

*Table 8: Summary of the final (MM) generalized additive model (GAM) for dissolved oxygen (DO): Parametric terms, smooth terms, k-check diagnostics, and significance. The table includes estimates and standard errors for parametric term depth class, as well as effective degrees of freedom (EDF), F-values, and p-values for smooth terms s(). Each smooth term is presented by regulation class (regulated vs. non-reg.) where applicable. Random effect (ID) is shown as random smoothers. Model diagnostics include the basis dimension used by the model (**k'**), the estimated EDF from the k-check (**EDF (k-check)**), the **k-index**, and the associated **K p-value**. A k-index close to 1 and a high K p-value suggest that the chosen basis dimension was sufficient, and the smooth was not underfitted.*

Term	Estimate	Std. Error	EDF	F	p-value	k'	EDF (k-check)	k-index	K p-value
(Intercept)	9.41	0.12		78.79	<0.001				
DEPTH CLASS 3-6m	0.11	0.18		0.60	0.552				
DEPTH CLASS 6-9m	0.65	0.38		1.72	**0.085**				
DEPTH CLASS >9m	0.23	0.38		0.61	0.542				
s(TEMPERATURE): NONREG			15.17	44.56	<0.001	19	15.17	0.96	0.01
s(TEMPERATURE): REGULATED			18.38	**3242.14**	<0.001	19	18.38	0.96	0.005
s(ID)			34.99	**4452.23**	<0.001	40	34.99		
s(ToD): NONREG			7.06	50.45	<0.001	22	7.06	0.99	0.4
s(ToD): REGULATED			10.36	**287.37**	<0.001	22	10.36	0.99	0.428
s(OUTLET): NONREG			1.00	0.05	0.834	29	1.00	0.95	<0.001
s(OUTLET): REGULATED			25.89	**110.22**	<0.001	29	25.89	0.95	<0.001
s(SPILL): NONREG			9.29	36.27	<0.001	29	9.29	0.97	0.013
s(SPILL):REGULATED			28.88	**500.97**	<0.001	29	28.88	0.97	0.013
s(TOT.Z. FLOW)			8.59	**50.33**	<0.001	9	8.59	1.00	0.562
s(DATE): NONREG			17.29	81.51	<0.001	19	17.29	0.96	0.013
s(DATE): REGULATED			18.87	**1732.92**	<0.001	19	18.87	0.96	0.002

4. Discussion

This study investigated the spatiotemporal variation of dissolved oxygen (DO) levels across 3 regulated and 2 free-flowing rivers in central and northern Sweden using a generalized additive model (GAM) framework. The objective was to evaluate whether river regulation significantly influences DO concentrations and to explore the additional effects of Site, time, flow, and depth on DO variability.

4.1 Role of regulation

The primary objective of this study was to assess whether regulated rivers show different levels of dissolved oxygen (DO) compared to non-regulated (free flowing) rivers, and to explore how these differences vary across space and time. The results clearly indicate that regulated rivers displayed distinct DO patterns compared to free-flowing rivers. In particular, the analysis revealed more frequent occurrences of extreme DO values in regulated rivers. This was supported by both variability metrics (standard deviation and coefficient of variation) and distribution shape metrics (skewness and kurtosis). Furthermore, variability metrics also suggested that regulated rivers are more prone to sudden changes in oxygen levels, such as sharp drops. A key feature observed in regulated rivers was a heavy-tailed distribution with a sharp peak near the median, and a long-left tail which suggested the higher frequency of extreme low DO values. In contrast, non-regulated rivers showed a more symmetrical and narrow distribution, indicating stable and consistent oxygen levels. This highlights that regulated systems are prone to extreme oxygen fluctuations during summer. This period often overlaps with higher average temperatures, lower precipitation, lower energy demand, thus likely longer water retention times, partly due to an increased occurrence of zero-flow events.

When examined at the individual river level, the same trends were present. Regulated rivers such as Luleälven, Umeälven, and Ljungan showed lower minimum DO values, which entailed moderate to severe hypoxia events in all of them. Although Ljungan showed a lower occurrence of extreme values compared to the other regulated rivers, all regulated systems experienced critical oxygen conditions, with concentrations falling below both moderate (5 mg/L) and severe (3 mg/L) hypoxia. In contrast, the free-flowing rivers had no DO values outside the optimal range (7 mg/l to 13 mg/l), further confirming the more stable oxygen conditions in unregulated systems.

Even though the average DO values were similar between regulated (mean= 9.4mg/l, median 9.4mg/l, S.E.=0.004) and unregulated rivers (mean= 9.7 mg/l, median 9.6 mg/l, S.E.=0.008), the higher frequency of low extremes in regulated rivers indicates a different and more stressful oxygen regime for aquatic life, which may entail serious ecological consequences, especially for sensitive species - such as Salmonids and sensitive macroinvertebrates- and impair key ecosystem processes (Diaz & Rosenberg 2008; Fusi et al. 2023). Further evidence of the impact of regulation on DO arise from the univariate model, which showed that regulated rivers had significantly lower DO levels overall. The model intercept was small (−0.183 mg/L), however the t-value = −24.9 provided sound statistical evidence that water regulation, for hydropower production, have a measurable negative effect on oxygen levels in the studied rivers.

It is important to note that while the average DO differences may appear small, the impact of extreme events carry a high ecological risk. These short but severe drops in oxygen can affect fish survival, macroinvertebrate diversity, and essential processes such as nutrient cycles (Pollock et al. 2007; Diaz & Rosenberg 2008; Ekau et al. 2010; Davie 2019b; Fusi et al. 2023). At a finer spatial scale, a high degree of variation was found between sampling sites. This highlights the higher diversity of conditions even within the same river system and justifies the inclusion of site ID as a random effect in the multivariate model, to account for local conditions and the related degree of unknown DO variation.

Again, dissolved oxygen is a key element in assessing physical and chemical water quality since it plays a crucial role in the functioning of freshwater ecosystems, influencing biological structure and processes such as respiration, decomposition, and nutrient dynamics. Along with other parameters like temperature, transparency, and nutrients, DO levels support aquatic flora and fauna and are used as indicators of ecological health. As well as, according to Annex V of the Water Framework Directive, DO is an essential parameter for assessing both ecological status in natural water bodies and ecological potential in Heavily Modified Water Bodies (HMWBs). In this study, the inspected bodies of water within the regulated rivers are officially classified as HMWBs with poor and bad ecological potential (table 9-13) meaning they fail to achieve the WFD target of "Good Ecological Potential". These findings highlight a critical situation for water chemistry in the studied HMWBs, particularly regarding dissolved oxygen conditions and the related consequences on the ecosystem.

The results also point out a lack of adequate monitoring framework as extreme low-oxygen events may go undetected under standard monitoring procedures due to ineffective temporal resolution. Finally, this study provides scientific evidence

of potential non-compliance with Articles 1 and 4 of the Water Framework Directive (WFD), which aim to prevent further deterioration of heavily modified water bodies (HMWBs) and to promote the achievement of good ecological potential. The repeated and extreme fluctuations in dissolved oxygen observed in regulated rivers may contribute to further ecological degradation, thereby exacerbating the already compromised condition of these ecosystems and undermining the objectives set out in the WFD.

4.2 Dissolved oxygen drivers

Multivariate GAMs showed that DO variation was mainly driven by sampling site (ID), temperature, and hydrological conditions, with clear differences between regulated and non-regulated rivers, displaying both spatial and temporal patterns. Sampling site (ID) resulted to be a significant factor ($p<0.001$) with a very strong effect over all ($F=4452.23$), suggesting high spatial heterogeneity, further supporting the inclusion of ID as random effect in the models. On the other hand, "River "and "Site" did not provide a significant improvement of the model suggesting that ID was already accounting for most of the unmodelled variation

Temperature also had a significant non-linear effect in both regulation classes, with a similar degree of complexity (EDF regulated=18.38; EDF nonregulated=15,17). Nevertheless, its influence on DO was much stronger in regulated systems ($F = 3242.14$) compared to non-regulated rivers ($F = 44.5$). The stronger effect in regulated rivers might arise from the fact that spill and outlet discharges draw water from different depths of the reservoirs, where thermal stratification is likely to occur during summer. This hypothesis is further supported by the fact that the univariate GAM model, which used temperature as response variable instead of DO, estimated an intercept of 16.49 °C in non-regulated rivers while regulated systems showed a statistically significant decrease of -0.42 °C (Estimate = –0.41555 °C; S.E. = 0.03078; t value = –13.5; $P<0.001$; n = 106,448), despite lower water velocity, higher retention times and lower shading.
Among the hydrological variables, spill and outlet discharge were major drivers of DO in regulated rivers, while they showed little or no effect in non-regulated rivers. Nevertheless, the smaller data range for discharge in non-regulated rivers may limit the reliability of this result. In contrast, the wider range of flow data in regulated rivers allows for a clearer understanding of how different flow types, as well as the absence of flow affect DO levels. Outlet discharge showed a significant effect in regulated rivers ($F = 110.22$; $p < 0.001$), although the model diagnostics indicated a slight underfit (k-index < 1) the outlet smooth function displayed higher fluctuation at lower discharge ($0< Q < 250$) values, and it showed an exponential increasing effect when discharge exceeded 250 m^3/s. Despite this, the overall outlet

effect remained relatively limited. Similarly, spill' smoother function of regulated rivers showed a higher degree of variation at lower discharge ($0< Q < 250$) values and a steady increasing effect at higher discharges ($Q > 300$ m^3/s). In non-regulated rivers, spill and outlet flow represent the same dataset due to occurrence of a single type of flow, (natural hydrological regime) typical of these systems. Thus, both flow types were based on a narrower data range and were associated with a wider error band, reflecting higher uncertainty in their estimated effects.

Notably, in regulated rivers, the partial effect of spill flow on the y axis was consistently higher than outlet discharge, as well as the higher F value (F=500.97) showed a bigger contribution of spill flow in explaining variation in the response, suggesting that spill flow has a greater aeration potential, likely caused by a turbulent flow condition which more closely resembles what naturally occur in shallow, fast-flowing, and highly turbulent stretches. This, also underlines the role of rapids as critical morphological features, as they may improve aeration capacity of river stretches by increasing the water surface in contact with the atmosphere (Cox 2003). Again, these features are almost entirely absent in regulated rivers, since the former elevation drop have been fully exploited for dam construction, and former rapids are now submerged beneath reservoirs or stand dry as bypass channels. Hence, these morphological modifications may have transformed the former lotic habitat into a cascade of lentic systems with deep, slow flowing water, resulting in a reduced re-aeration potential as well as a direct loss of habitat.

The absence of flow (zero flow) showed a significant non-linear effect in regulated rivers ($F=50.33$; $p < 0.001$), the only regulation class where zero flow occurred. The smoother function showed allow degree of complexity (EDF=8.59), with a slightly increasing trend, followed by a steady decline in DO as zero flow duration increased. This provides further evidence that zero flow events can directly impact DO levels, with longer durations leading to increasingly low oxygen concentrations. The high variability of zero flow effect at short duration reflect the high unpredictability of flow fluctuation which seemed to occur mor frequently at relatively low discharge. Date also explained a significant amount of temporal variability in dissolved oxygen (DO) in both regulation classes ($p < 0.001$). While in the free-flowing rivers the partial effect fluctuated around zero and the factor's contribution was relatively limited ($F = 81.51$), in regulated rivers the smooth function showed a decreasing trend toward the end of summer, with the smooth term strongly contributing ($F=1732.92$) to explaining variation in the response. The greater degree of temporal variability highlighted by the model in regulated rivers again suggests a strong relationship between DO dynamics and hydropower operations.

Similarly, time of day (ToD) explained a significant portion of the variation in the response across both regulation classes showing again a stronger contribution in regulated rivers (F = 287.37) and slightly higher complexity (EDF = 10.36) compared to non-regulated rivers (F = 50.45, EDF = 7.06). As expected, dissolved oxygen followed a clear daily cycle as indicated by the smooth term, reflecting the varying balance between photosynthesis and respiration during daylight and nighttime hours. The higher complexity and stronger association of the predictor with DO in regulated river suggested a higher degree of variability in the daily oxygen cycles of oxygen, likely driven by hydropower operations. Lastly, depth showed a weaker and non-significant influence on dissolved oxygen. However, mid-range depths (6–9 m) exhibited a marginal positive effect (estimate = 0.65, p = 0.085) compared to the reference class (0–3 m) suggesting a weak trend toward higher oxygen levels. These results might potentially indicate a reduced vertical mixing capacity in regulated systems, where this depth class was exclusively observed. This hypothesis is further validated by the higher fluctuation of DO levels in the class 0-3m and by the temporal variation which also suggest presence of poor mixing capacity during summer months. Nevertheless, the role of depth in these systems remains poorly understood and warrants further investigation.

These findings underline significant differences in dissolved oxygen (DO) dynamics between regulated and non-regulated rivers, emphasizing the strong influence of hydropower operations and associated morphological and hydrological alterations. While natural systems exhibit more stable spatial and temporal oxygen patterns, regulated rivers displayed higher variability, mostly driven by highly variable discharge regimes, and impaired aeration potential. This highlights the need for further research and emphasizes the potential of adaptive flow management, such as implementing environmental flow (e-Flow) measures that utilize a substantial release of discharge through the spillway. These measures could help reactivate bypass channels, thereby partially compensating for the loss of critical morphological features like riffles and rapids. Moreover, where reactivation of former morphology is not feasible, active restoration of these features should be undertaken. Additionally, improving water management through inclusion of water quality objectives into hydropeaking models should be prioritized to mitigate impact on Dissolved oxygen dynamics under growing energy demand and climatic pressures. Collectively, these measures could support the maintenance of adequate DO levels, enhance aquatic ecosystem health, reduce the ecological footprint of hydropower infrastructure, and contribute to achieving a good ecological potential.

4.3 Caveats and Future monitoring

The substantially higher number of observations in regulated rivers (N = 97153) compared to non-regulated ones (N = 9295) likely resulted in biasing model outputs, potentially inflating the perceived influence of covariates within the regulated class. Additionally, the concentrated sampling effort in a single river system (Ljungan) may have exacerbated this imbalance, further limiting the generalizability of the results. The uneven distribution of transects across rivers and sites could also have led to underestimation of depth-related effects, potentially hiding patterns associated with seasonal thermal stratification. Moreover, since transects were conducted only in lakes and not in reservoirs, the study could not directly assess thermal stratification processes specific to reservoirs. Another issue that arose was the high variability and not clear definition of zero-flow events, which prevent an accurate calculation of their duration and the consequent flow condition at sampling location. This subtle mismatch may have contributed to add uncertainty in the model predictions related to flow-dependent variables especially concerning duration of zero flow events.

Furthermore, all loggers were placed relatively close to the bottom, while necessary, this may have introduced additional bias, particularly regarding vertical variability within the water column. To address these limitations, future research and monitoring plans should aim for a more representative spatial distribution of sampling sites across regulation classes and river systems to reduce overrepresentation and improve comparability. Improving transect design, such as standardizing depth intervals and exploring their relationship with temperature and dissolved oxygen would enhance the study of vertical stratification processes, particularly in reservoirs. Additionally, a clear understanding of the local flow condition at each the sampling site is essential to improve model accuracy and better explore the effect of flow condition, especially zero flow events and their duration.

4.4 Adaptive management and the Water framework directive

According to Annex V, section 1.3.4 of the Water Framework Directive, operational monitoring must provide sufficient data for a reliable assessment of water body status, with a frequency that minimizes the influence of natural variability (e.g. daily, seasonal fluctuations) to better capture changes driven by human pressures. Given that the minimum sampling interval for operational monitoring of Physico-chemical quality element, specifically “Oxygenation”, should be taken at intervals not exceeding three months, the temporal variability of dissolved oxygen detected in this study, particularly in regulated rivers, strongly

supports the need for high time-resolution surveys to ensure confident, precise, and representative assessments of DO condition in the bodies of water. As well as the high spatial variability and the lack of a clear understanding of why and where hypoxic events occur, stressed the need of site-specific DO conditions assessment for each individual HMBWs. Moreover, since the reasons of extreme Dissolved oxygen variation remain unknown, Investigative monitoring shall be carried out according to section 1.3.3. “Desing of Investigative monitoring “, thus make using this pilot study as base to develop and test further hypothesis and experiments.

4.5 Conclusion

This study is among the few to investigate dissolved oxygen dynamics at an hourly resolution in both regulated and non-regulated rivers, while also exploring correlations with hydropower operations, including different types of discharge and zero-flow events. DO plays a pivotal role in supporting aquatic biodiversity, as it directly influences metabolic processes, species distribution, and overall ecosystem health. Impairments in DO levels, particularly frequent or prolonged periods of low oxygen can have serious consequences for freshwater biodiversity, especially for oxygen-sensitive species. These findings highlight the need for further investigations into the spatial extent of DO extremes events and their ecological consequences, particularly regarding its impact on biodiversity in regulated systems.

References

BUNN, S.E. & ARTHINGTON, A.H. (2002). Basic Principles and Ecological Consequences of Altered Flow Regimes for Aquatic Biodiversity. *Environmental Management*, 30 (4), 492–507. https://doi.org/10.1007/s00267-002-2737-0

Calapez, A.R., Branco, P., Santos, J.M., Ferreira, T., Hein, T., Brito, A.G. & Feio, M.J. (2017). Macroinvertebrate short-term responses to flow variation and oxygen depletion: A mesocosm approach. *Science of The Total Environment*, 599–600, 1202–1212. https://doi.org/10.1016/j.scitotenv.2017.05.056

COMMISSION STAFF WORKING DOCUMENT Third River Basin Management Plans Second Flood Hazard and Risk Maps and Second Flood Risk Management Plans Member State: Sweden Accompanying the document REPORT FROM THE COMMISSION TO THE COUNCIL AND THE EUROPEAN PARLIAMENT on the implementation of the Water Framework Directive (2000/60/EC) and the Floods Directive (2007/60/EC) Third River Basin Management Plans Second Flood Risk Management Plans (2025). . https://eur-lex.europa.eu/legal-content/EN/TXT/?uri=SWD%3A2025%3A22%3AFIN&qid=1738746144581 [2025-02-11]

Cox, B. (2003). A review of dissolved oxygen modelling techniques for lowland rivers. *The Science of The Total Environment*, 314–316, 303–334. https://doi.org/10.1016/S0048-9697(03)00062-7

Davie, T. (2019a). *Fundamentals of Hydrology*. 3rd ed. Routledge. (Routledge Fundamentals of Physical Geography Ser)

Davie, T. (2019b). *Fundamentals of Hydrology*. 3rd ed. Routledge. (Routledge Fundamentals of Physical Geography Ser)

Diaz, R.J. & Rosenberg, R. (2008). Spreading dead zones and consequences for marine ecosystems. *Science (New York, N.Y.)*, 321 (5891), 926–929. https://doi.org/10.1126/science.1156401

Directive 2000/60/EC (2000). . https://eur-lex.europa.eu/eli/dir/2000/60/oj

Dynesius, M. & Nilsson, C. (1994). Fragmentation and Flow Regulation of River Systems in the Northern Third of the World. *Science*, 266 (5186), 753–762. https://doi.org/10.1126/science.266.5186.753

Ekau, W., Auel, H., Pörtner, H.-O. & Gilbert, D. (2010). Impacts of hypoxia on the structure and processes in pelagic communities (zooplankton, macro-invertebrates and fish). *Biogeosciences*, 7 (5), 1669–1699. https://doi.org/10.5194/bg-7-1669-2010

Fusi, M., Rigaud, S., Guadagnin, G., Barausse, A., Marasco, R., Daffonchio, D., Régis, J., Huchet, L., Camin, C., Pettit, L., Vina-Herbon, C. & Giomi, F. (2023). Ideas and perspectives: The fluctuating nature of oxygen shapes the ecology of aquatic habitats and their biogeochemical cycles – the aquatic oxyscape. *Biogeosciences*, 20 (16), 3509–3521. https://doi.org/10.5194/bg-20-3509-2023

Grill, G., Lehner, B., Thieme, M., Geenen, B., Tickner, D., Antonelli, F., Babu, S., Borrelli, P., Cheng, L., Crochetiere, H., Ehalt Macedo, H., Filgueiras, R., Goichot, M., Higgins, J., Hogan, Z., Lip, B., McClain, M.E., Meng, J., Mulligan, M., Nilsson, C., Olden, J.D., Opperman, J.J., Petry, P., Reidy Liermann, C., Sáenz, L., Salinas-Rodríguez, S., Schelle, P., Schmitt, R.J.P., Snider, J., Tan, F., Tockner, K., Valdujo, P.H., van Soesbergen, A. & Zarfl, C. (2019). Mapping the world's free-flowing rivers. *Nature*, 569 (7755), 215–221. https://doi.org/10.1038/s41586-019-1111-9

HOBO Dissolved Oxygen Logger (U26-001) Manual (s.d.).

Jansson, R., Nilsson, C., Dynesius, M. & Andersson, E. (2000). Effects of River Regulation on River-Margin Vegetation: A Comparison of Eight Boreal Rivers. *Ecological Applications*, 10 (1), 203–224. https://doi.org/10.1890/1051-0761(2000)010[0203:EORROR]2.0.CO;2

Kallis, G., Hickel, J., O'Neill, D.W., Jackson, T., Victor, P.A., Raworth, K., Schor, J.B., Steinberger, J.K. & Ürge-Vorsatz, D. (2025). Post-growth: the science of wellbeing within planetary boundaries. *The Lancet Planetary Health*, 9 (1), e62–e78. https://doi.org/10.1016/S2542-5196(24)00310-3

Lakowicz, J.R. (a c. di) (2006). Quenching of Fluorescence. In: *Principles of Fluorescence Spectroscopy*. Springer US. 277–330. https://doi.org/10.1007/978-0-387-46312-4_8

Lytle, D.A. & Poff, N.L. (2004). Adaptation to natural flow regimes. *Trends in Ecology & Evolution*, 19 (2), 94–100. https://doi.org/10.1016/j.tree.2003.10.002

MX800 Series User Guide | Onset's HOBO Data Loggers (s.d.). https://www.onsetcomp.com/resources/documentation/mx800-series-user-guide?srsltid=AfmBOoqnhbcPXg4eL0FfRAe-9CfPw4Jx5HL6oRSMx7bS-Smdtn2-pRt6 [2025-03-27]

Nilsson, C., Reidy, C.A., Dynesius, M. & Revenga, C. (2005). Fragmentation and Flow Regulation of the World's Large River Systems. *Science*, 308 (5720), 405–408. https://doi.org/10.1126/science.1107887

Parasiewicz, P., Belka, K., Łapińska, M., Ławniczak, K., Prus, P., Adamczyk, M., Buras, P., Szlakowski, J., Kaczkowski, Z., Krauze, K., O'Keeffe, J., Suska, K., Ligięza, J., Melcher, A., O'Hanley, J., Birnie-Gauvin, K., Aarestrup, K., Jones, P.E., Jones, J., Garcia de Leaniz, C., Tummers, J.S., Consuegra, S., Kemp, P., Schwedhelm, H., Popek, Z., Segura, G., Vallesi, S., Zalewski, M. & Wiśniewolski, W. (2023). Over 200,000 kilometers of free-flowing river habitat in Europe is altered due to impoundments. *Nature Communications*, 14 (1), 6289. https://doi.org/10.1038/s41467-023-40922-6

Pebesma, E. & Bivand, R. (2023). *Spatial Data Science: With Applications in R*. Chapman and Hall/CRC. https://doi.org/10.1201/9780429459016

Pedersen, E.J., Miller, D.L., Simpson, G.L. & Ross, N. (2019). Hierarchical generalized additive models in ecology: an introduction with mgcv. *PeerJ*, 7, e6876. https://doi.org/10.7717/peerj.6876

Poff, N. & Allan, J.D. (1995). Functional Organization of Stream Fish Assemblages in Relation to Hydrologic Variability. *Ecology*, 76. https://doi.org/10.2307/1941217

Poff, N. & Ward, J. (1990). Physical habitat template of lotic systems: Recovery in the context of historical pattern of spatiotemporal heterogeneity. *Environmental Management*, 14, 629–645. https://doi.org/10.1007/BF02394714

Poff, N.L., Allan, J.D., Bain, M.B., Karr, J.R., Prestegaard, K.L., Richter, B.D., Sparks, R.E. & Stromberg, J.C. (1997). The Natural Flow Regime. *BioScience*, 47 (11), 769–784. https://doi.org/10.2307/1313099

Poff, N.L. & Zimmerman, J.K.H. (2010). Ecological responses to altered flow regimes: a literature review to inform the science and management of environmental flows. *Freshwater Biology*, 55 (1), 194–205. https://doi.org/10.1111/j.1365-2427.2009.02272.x

Pollock, M.S., Clarke, L.M.J. & Dubé, M.G. (2007). The effects of hypoxia on fishes: from ecological relevance to physiological effects. *Environmental Reviews*, 15 (NA), 1–14. https://doi.org/10.1139/a06-006

Quaranta, E., Aggidis, G., Boes, R.M., Comoglio, C., De Michele, C., Ritesh Patro, E., Georgievskaia, E., Harby, A., Kougias, I., Muntean, S., Pérez-Díaz, J., Romero-Gomez, P., Rosa-Clot, M., Schleiss, A.J., Vagnoni, E.,

Wirth, M. & Pistocchi, A. (2021). Assessing the energy potential of modernizing the European hydropower fleet. *Energy Conversion and Management*, 246, 114655. https://doi.org/10.1016/j.enconman.2021.114655

{R Core Team} (2024). *R: A Language and Environment for Statistical Computing* (R version 4.3.3). R Foundation for Statistical Computing. https://www.R-project.org/

RENEWABLES 2023 GLOBAL STATUS REPORT (s.d.). https://www.ren21.net/gsr-2023/ [2025-02-11]

Stewardson, M.J., Acreman, M., Costelloe, J.F., Fletcher, T.D., Fowler, K.J.A., Horne, A.C., Liu, G., McClain, M.E. & Peel, M.C. (2017). Understanding Hydrological Alteration. In: *Water for the Environment*. Elsevier. 37–64. https://doi.org/10.1016/B978-0-12-803907-6.00003-6

Sweden - Countries & Regions (s.d.). *IEA*. https://www.iea.org/countries/sweden [2025-02-13]

Warren, M., Dunbar, M.J. & Smith, C. (2015). River flow as a determinant of salmonid distribution and abundance: a review. *Environmental Biology of Fishes*, 98 (6), 1695–1717. https://doi.org/10.1007/s10641-015-0376-6

Wentworth, C.K. (1922). A Scale of Grade and Class Terms for Clastic Sediments. *The Journal of Geology*, 30 (5), 377–392

Wetzel, R.G. (2001). *Limnology: Lake and River Ecosystems*. Gulf Professional Publishing.

Wickham, H., Averick, M., Bryan, J., Chang, W., McGowan, L., François, R., Grolemund, G., Hayes, A., Henry, L., Hester, J., Kuhn, M., Pedersen, T., Miller, E., Bache, S., Müller, K., Ooms, J., Robinson, D., Seidel, D., Spinu, V. & Yutani, H. (2019). Welcome to the Tidyverse. *Journal of Open Source Software*, 4, 1686. https://doi.org/10.21105/joss.01686

Widén, Å., Renöfält, B.M., Degerman, E., Wisaeus, D. & Jansson, R. (2021). Let it flow: Modeling ecological benefits and hydropower production impacts of banning zero-flow events in a large regulated river system. *Science of The Total Environment*, 783, 147010. https://doi.org/10.1016/j.scitotenv.2021.147010

WISE EIONET Spatial Datasets (s.d.). https://www.eea.europa.eu/en/datahub/datahubitem-view/c2c99dcc-ebe2-4dd7-9248-0219a82f6eb3 [2025-04-05]

Wood, S.N. (2017). *Generalized Additive Models: An Introduction with R, Second Edition*. 2. ed. Chapman and Hall/CRC. https://doi.org/10.1201/9781315370279

Popular science summary

The gagged rivers

When we think of breathing, we often picture animals with lungs, but did you know that fish, insects, and even bacteria breathe too, even underwater?

In aquatic ecosystems, oxygen is present in the form of dissolved oxygen (DO), that simply is oxygen molecules mixed into the water. This mainly comes from photosynthesis by aquatic plants and aeration, the process where air mixes with water. This happens especially in fast-flowing stretches which are usually rich in oxygen making this oxygen-rich areas vital habitats for species like salmon and trout, which depend well-oxygenated water to survive.

So, water flow isn't just about movement it's a key part of the life cycle of aquatic organisms. From salmon to mayflies, and even aquatic plants, many species are adapted to the natural rise and fall of river flows throughout the year, as well as flowing water transports nutrients and helps shape the habitats where these species live.

Hydropower produces energy from flowing water and is the world's most common source of renewable energy. Its popularity is due to a low carbon footprint and a good flexibility in energy production. In Sweden, hydropower provides around 40% of the country's electricity, making it the largest source of electric energy for the country.

However, hydropower isn't without costs. Dams and flow regulation can disrupt natural water movement, affect the life cycles of aquatic organisms, as well as reduce water velocity and mixing can negatively impact oxygen levels. One common hydropower method is called hydropeaking and consists in fast and short fluctuation of water flow, to match electricity demand and price. Sometimes, this also leads to periods of "zero flow," when water stops flowing downstream a hydropower station.

My study looked at five Swedish rivers, comparing regulated (hydropower-affected) and unregulated (free-flowing) systems. I found that regulated rivers tend to have lower oxygen levels than unregulated ones and are more prone to frequent and extreme fluctuations in oxygen, sometimes dropping to dangerously low levels. In contrast, free-flowing rivers showed more stable and higher oxygen concentrations, creating better living conditions for oxygen-sensitive species.

Interestingly, I also found that oxygen levels vary widely from site to site.

In regulated rivers, fluctuations in DO were strongly linked to hydropower operations, especially the release of "spill" water, which behaves more like natural rapids and helps increase oxygen levels. Similarly, DO was also influenced by the duration of zero-flow events showing that stopping the low for longer period worsen oxygen conditions. Healthy freshwater ecosystems need well-oxygenated water, and this study highlights the importance of improving hydropower water management to reduce its ecological impacts, especially considering the future need of renewable energy production in the face of climate change.

In short, to protect the rivers and the life within them, we need to balance efficiency and revenue with the limits of natural systems, making hydropower a real sustainable and low impact energy source.

Appendix

Supplementary tables

*Table 9: Table of sampling sites located along Umeälven. The table provides details for each sampling location, such as logger ID, site name, water body name according to **WISE** dataset and the relative **VISS code** (Vatteninformationnssystem Sverige), origin (Heavily Modified = HM), ecological potential, and site classification. Note that site classification is defined specifically for the purposes of this study and does not correspond to the WISE/VISS system.*

Logger ID	Water body (WISE)	VISS EU_CD	Origin	Ecol. potential	Site	Hp. upstream	Hp. downstream
UMP001	mellan Forsnacken och Slussfors	SE725821-151899	HM	Poor	River	Gardikforsen	Umpluspen
UMP002	mellan Långselet och Barselet	SE721599-157420	HM	Poor	River	Stensele	Grundfors
UMP003	Bjurfors Nedre dämningsområde	SE711610-168330	HM	Poor	Reservoir	Bjufors Ovre	Bjufors Nedre
UMP004	Harrsele dämningsområde	SE710657-168369	HM	Poor	Reservoir	Bjufors Nedre	Harrsele
UMP005	Pengfors dämningsområde	SE709720-168910	HM	Poor	Reservoir	Harrsele	Pengfors
UMP006	Umeälven	SE708620-171973	HM	Moderate	River	Stornorrfors	NA

*Table 10: Table of sampling sites located along Vindelälven. The table provides details for each sampling location, such as logger ID, site name, water body name according to **WISE** dataset and the relative **VISS code** (Vatteninformationnssystem Sverige), origin, ecological status, and site classification. Note that site classification is defined specifically for the purposes of this study and does not correspond to the WISE/VISS system*

Logger ID	Water body (WISE)	VISS EU_CD	Origin	Ecol. status	Site	SMHI Station ID
VIP001	Vindelälven	SE723591-161219	Natural	Good	River	2238
VIP002	Vindelälven	SE718190-165882	Natural	Good	River	2238
VIP003	Vindelälven	SE718190-165882	Natural	Good	River	2238
VIP004	Vindelälven	SE718190-165882	Natural	Good	River	2237

*Table 11: Table of sampling sites located along Piteälven. The table provides details for each sampling location, such as logger ID, site name, water body name according to **WISE** dataset and the relative **VISS code** (Vatteninformationnssystem Sverige), origin, ecological status, and site classification. Note that site classification is defined specifically for the purposes of this study and does not correspond to the WISE/VISS system*

Logger ID	Water body (WISE)	VISS EU_CD	Origin	Ecol. status	Site	SMHI Station ID
PIP002	Övre Trollselet	SE732858-165789	Natural	Good	River	1387
PIP001	Piteälven	SE732002-167678	Natural	Good	River	1387

*Table 12: Table of sampling sites located along Luleälven. The table provides details for each sampling location, such as logger ID, site name, water body name according to **WISE** dataset and the relative **VISS code** (Vatteninformationnssystem Sverige), origin (Heavily Modified = HM), ecological potential, and site classification. Note that site classification is defined specifically for the purposes of this study and does not correspond to the WISE/VISS system.*

Logger ID	Water body (WISE)	VISS EU_CD	Origin	Ecol. potential	Site	Hp. upstream	Hp.downstream
LUP001	Porjusselet	SE743475-167467	HM	Poor	Reservoir	NA	Porjus
LUP002	Harsprångsselet	SE742666-167549	HM	Poor	Reservoir	Porjus	Harsprånget
LUP003	Ligga-Dämningsområde	SE741849-167985	HM	Poor	Reservoir	Harsprånget	Ligga
LUP004	Messauremagasinet	SE740537-169963	HM	Bad	Reservoir	Ligga	Messaure
LUP005	Luleälven	SE739919-170400	HM	Poor	River	Messaure	Porsi
LUP009	Porsidammen	SE737840-171613	HM	Poor	Outlet	Messaure	Porsi
LUP008	Letsimagasinet	SE738541-170338	HM	Poor	Reservoir	Akkats	Letsi
LUP007	Letsimagasinet	SE738541-170338	HM	Poor	Reservoir	Akkats	Letsi
LUP010	Finnselet	SE735635-172734	HM	Poor	Reservoir	Porsi	Laxede
LUP006	Luleälven	SE730636-177276	HM	Poor	Outlet	Boden	NA

*Table 13: Table of sampling sites located along Ljungan. The table provides details for each sampling location, such as logger ID, site name, water body name according to **WISE** dataset and the relative **VISS code** (Vatteninformationnssystem Sverige), origin (Heavily Modified = HM), ecological potential, and site classification. Note that site classification is defined specifically for the purposes of this study and does not correspond to the WISE/VISS system.*

Logger ID	Water body (WISE)	VISS EU_CD	Origin	Ecol. Potential/status	Site	Hp. upstream	Hp.downstream
LJP001	Ljungan	SE691018-157875	Natural	Moderate	Outlet	Viforsen	NA
LJTa*	Marmen	SE691174-157065	Natural	Moderate	River	Matfors	Viforsen
LJP004	Marmen	SE691174-157065	Natural	Moderate	Lake	Matfors	Viforsen
LJTb*	Marmen	SE691174-157065	Natural	Moderate	Lake	Matfors	Viforsen
LJP009	Matfors - Marmen	SE691427-156408	HM	Poor	River	Matfors	Viforsen
LJP007	Skallböle - Matfors	SE691700-156189	HM	Poor	Reservoir	Skallböle	Matfors
LJP008	Skallböle - Matfors	SE691700-156189	HM	Poor	Outlet	Skallböle	Matfors
LJP018	Översjön / Ljungan	SE692463-145587	Natural	Moderate	Reservoir	Turinge	Bursnas
LJP017	Översjön / Ljungan	SE692463-145587	Natural	Moderate	River	Turinge	Bursnas

LJP012	Ljungan nedströms Handsjön	SE692800-144863	HM	Poor	Res.	Ratans	Turinge
LJP011	Handsjön	SE692897-144734	HM	Poor	Lake	Ratans	Turinge
LJP014	Handsjön	SE692897-144734	HM	Poor	Lake	Ratans	Turinge
LJP016	Rätanssjön	SE693109-143914	HM	Poor	Res.	Trangfors	Ratans
LJP015	Rätanssjön	SE693109-143914	HM	Poor	Lake	Trangfors	Ratans
LJTc*	Rätanssjön	SE693109-143914	HM	Poor	Lake	Trangfors	Ratans
LJP019	mellan Nästelsjönoch Rätanssjön	SE693587-143096	Natural	Poor	River	Trangfors	Ratans
LJP020	Nästelsjön	SE693816-143164	Natural	Poor	River	Trangfors	Ratans
LJPRF	Över-Grucken	SE697089-137693	Natural	Poor	River	NA	Flasjo

Supplementary figures

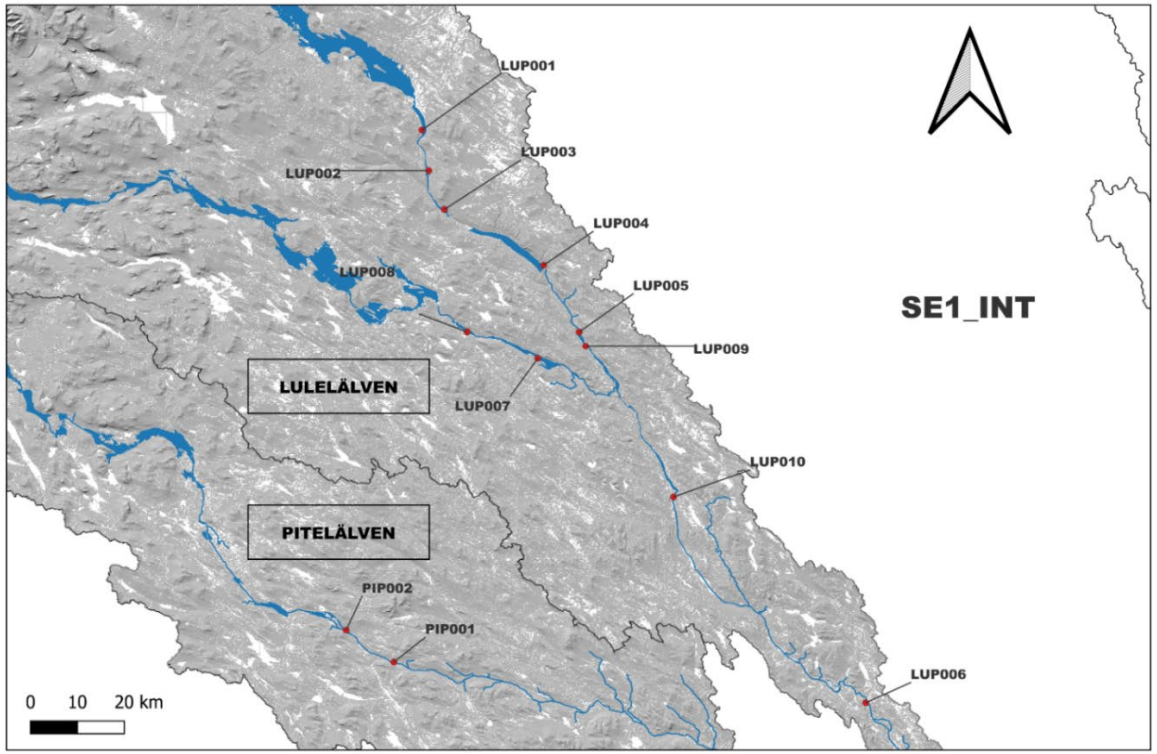

Figure 11: Map of sampling sites along Luleälven and Piteälven. This map is a "zoom in" of figure 2

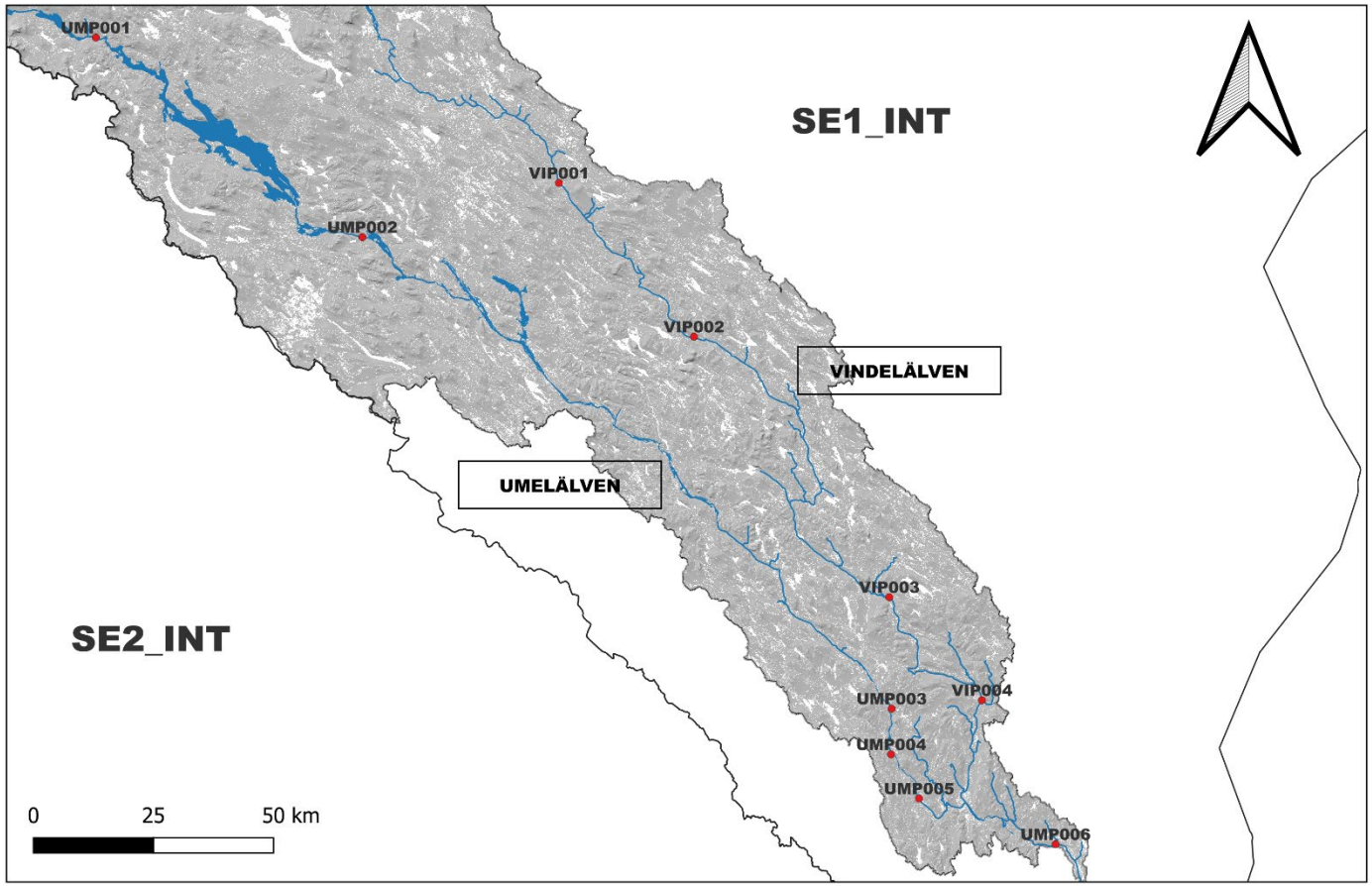

Figure 12: Map of sampling sites along Vindelälven and Umeälven. This map is a "zoom in" of figure 2

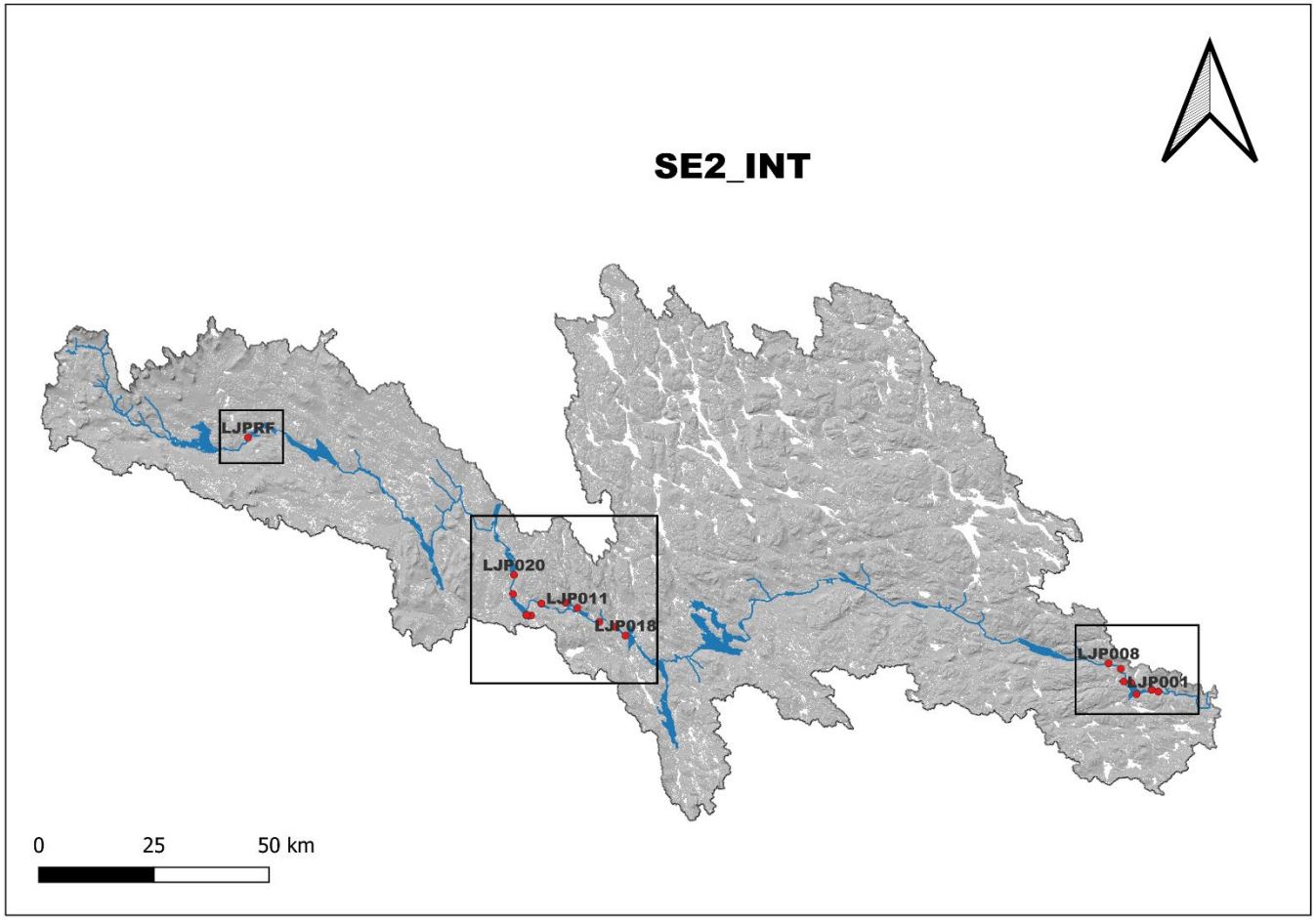

Figure 13: Map of sampling sites along Ljungan. This map is a "zoom in" of figure 2 higher resolution of sampling sites in figure 14

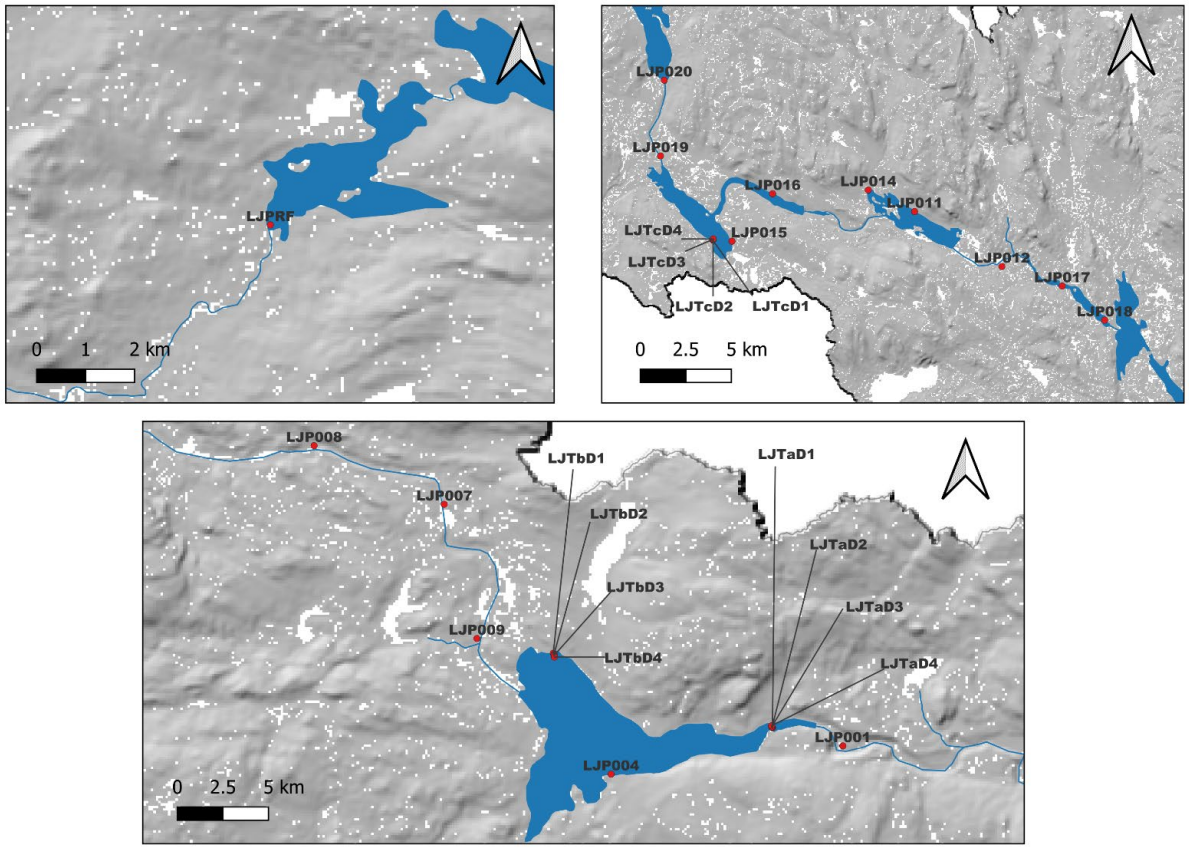

Figure 14: Higher resolution of sampling sites in Ljungan.

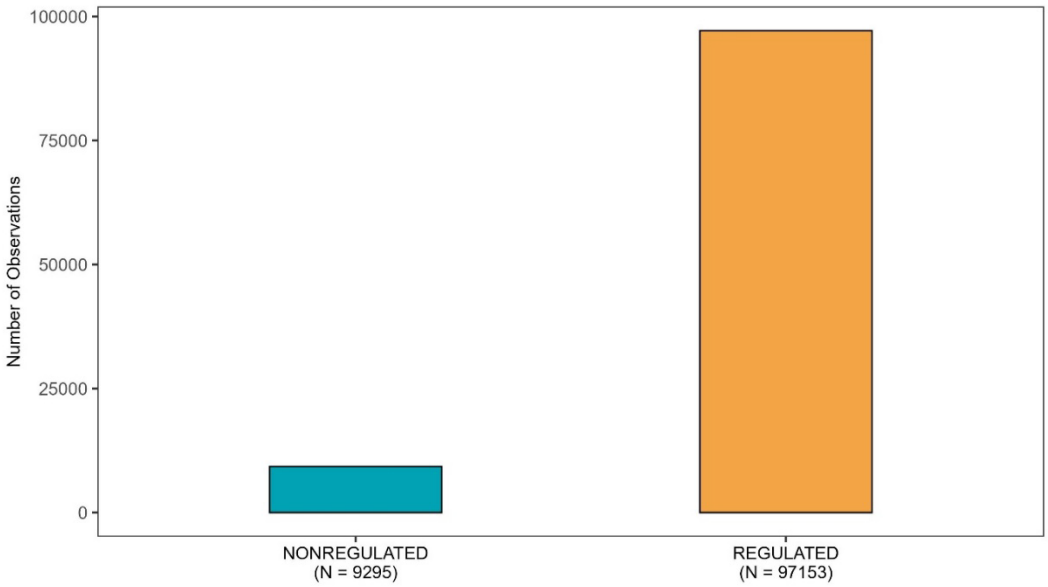

Figure 15: Number of observations by regulation class. The bar plot shows the number of observations across regulation classes (regulated vs. non-regulated) illustrating the sampling effort and the experimental design of the study 2024

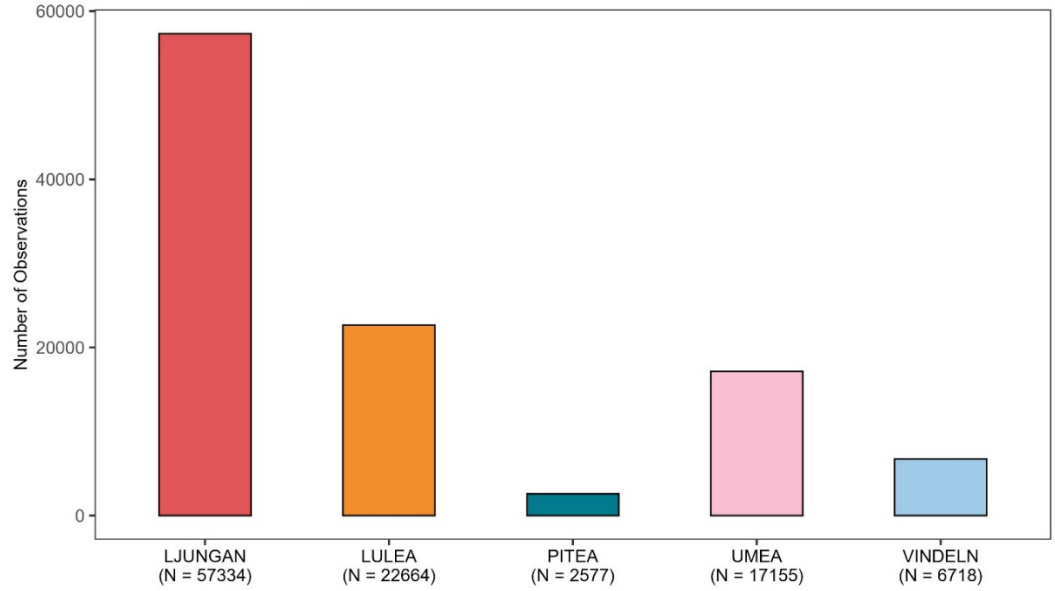

Figure 16: Number of observations by river. The bar plot shows the number of observations across rivers illustrating the sampling effort and the experimental design of the study 2024

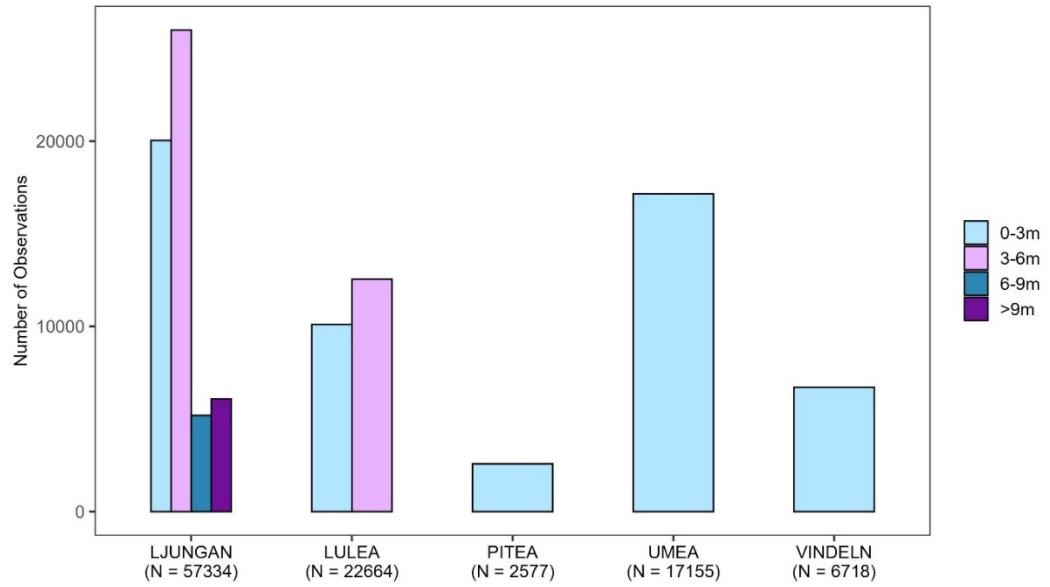

Figure 17: Number of observations by depth class. The bar plot shows the number of observations across depth classes illustrating the sampling effort and the experimental design of the study 2024

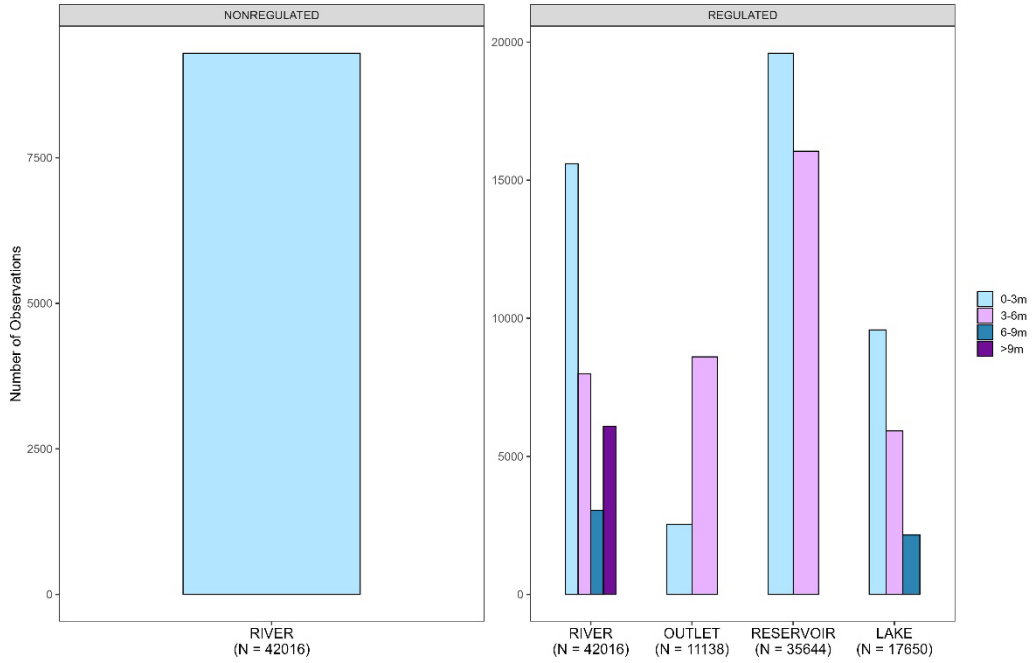

Figure 18: Number of observations by site and depth class across regulation classes (regulated & nonregulated). Bar plot illustrating the sampling effort and the experimental design of the study 2024

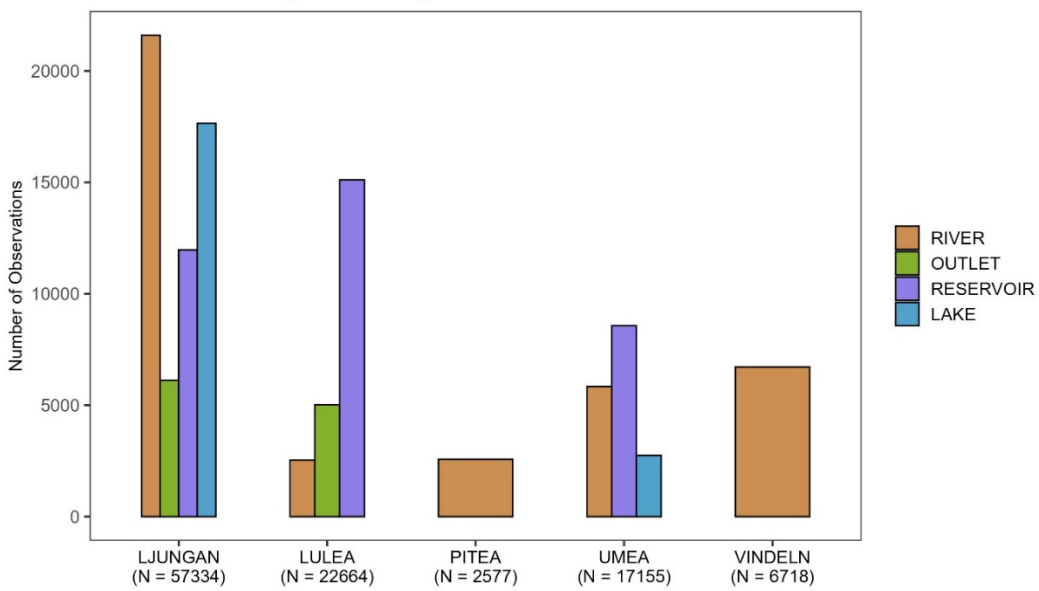

Figure 19: Number of observations by sites across rivers. Bar plot illustrating the sampling effort and the experimental design of the study 2024

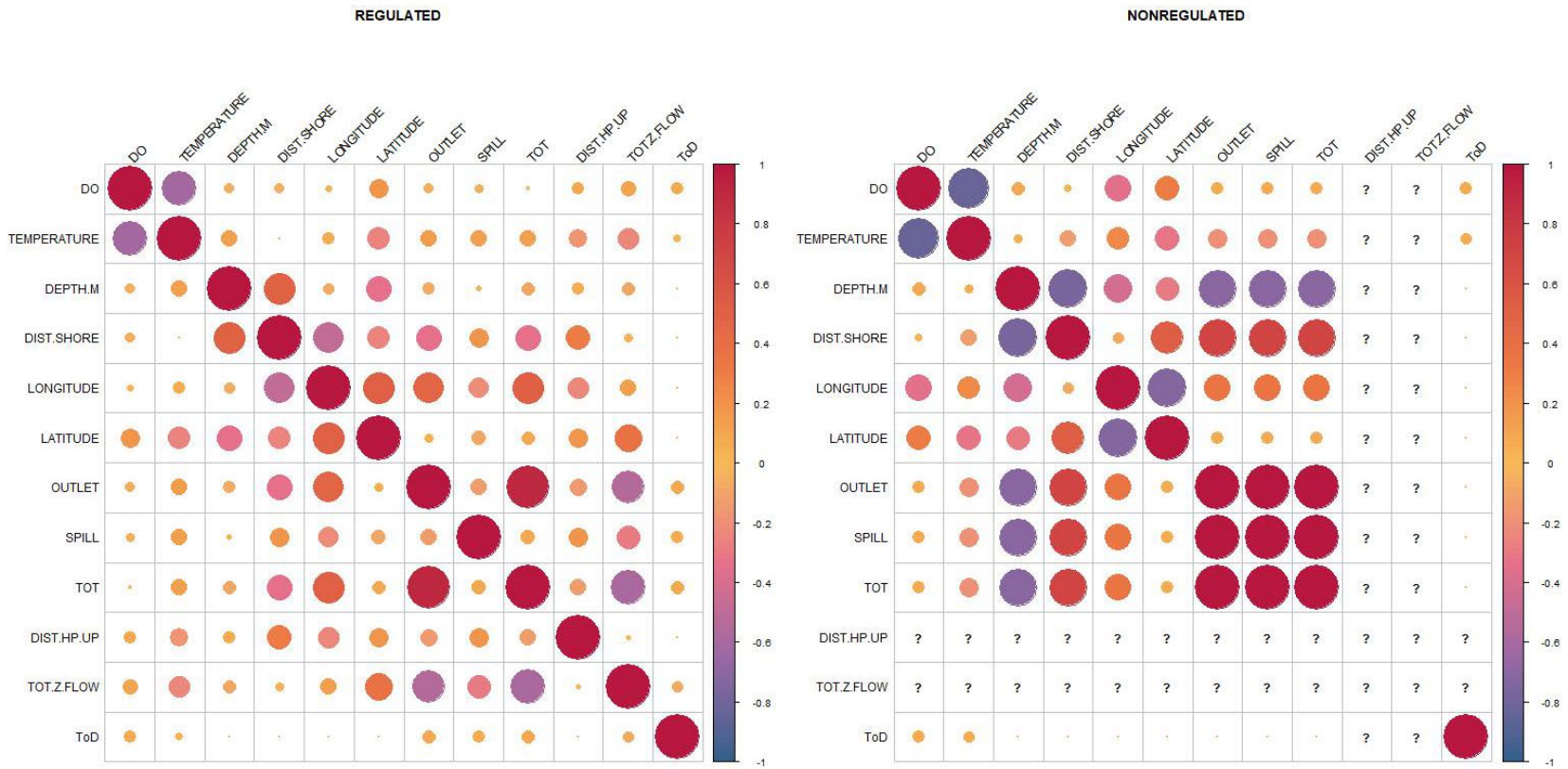

Figure 20: Correlation matrix of predictors. The matrix displays pairwise Spearman correlation coefficients between predictor variables across regulation classes used in the model selection. Colours and values indicate the strength and direction of the relationships as shown in the side bar.

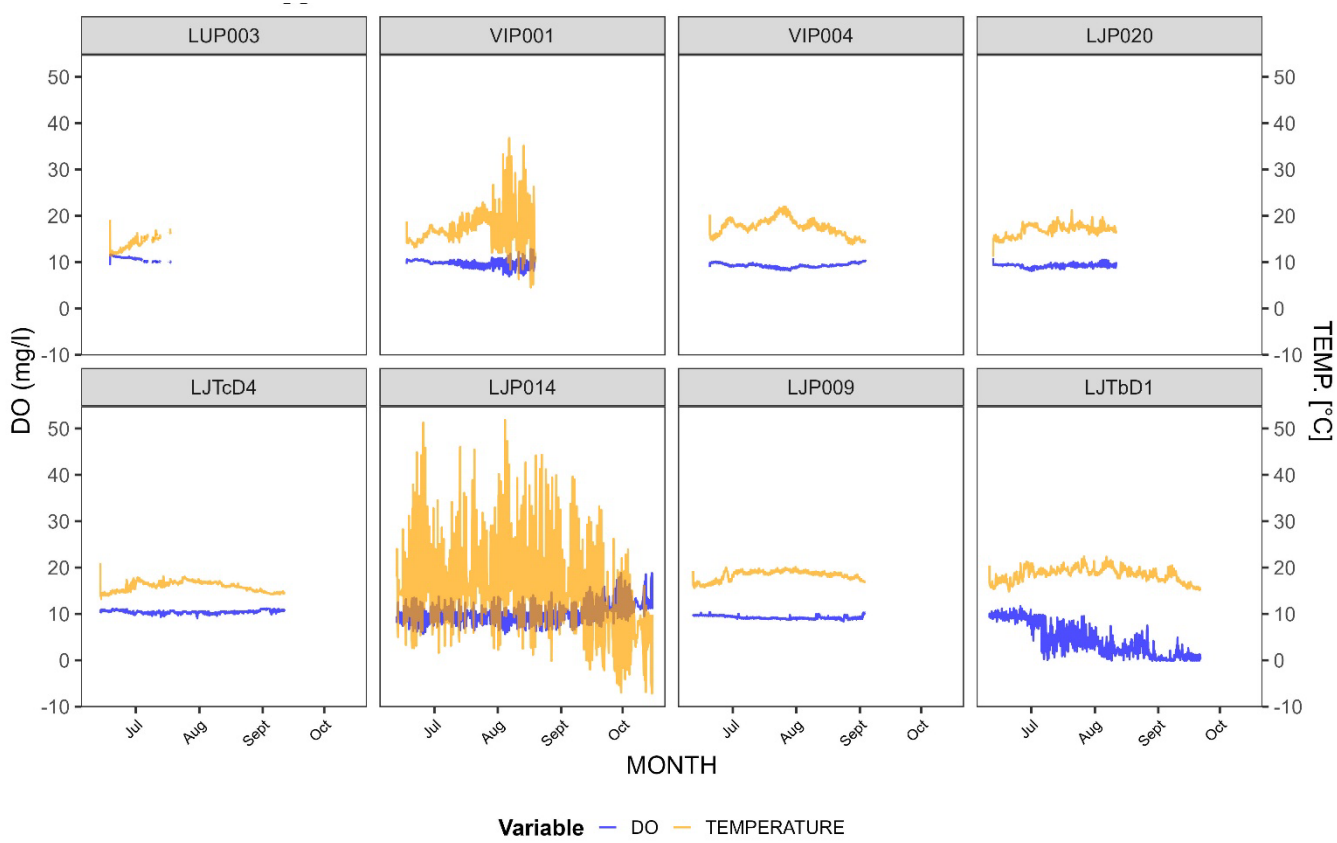

Figure 21: Problematic loggers' measurements of dissolved oxygen (blue) and Temperature (yellow) plotted as row data to visually assess data quality.

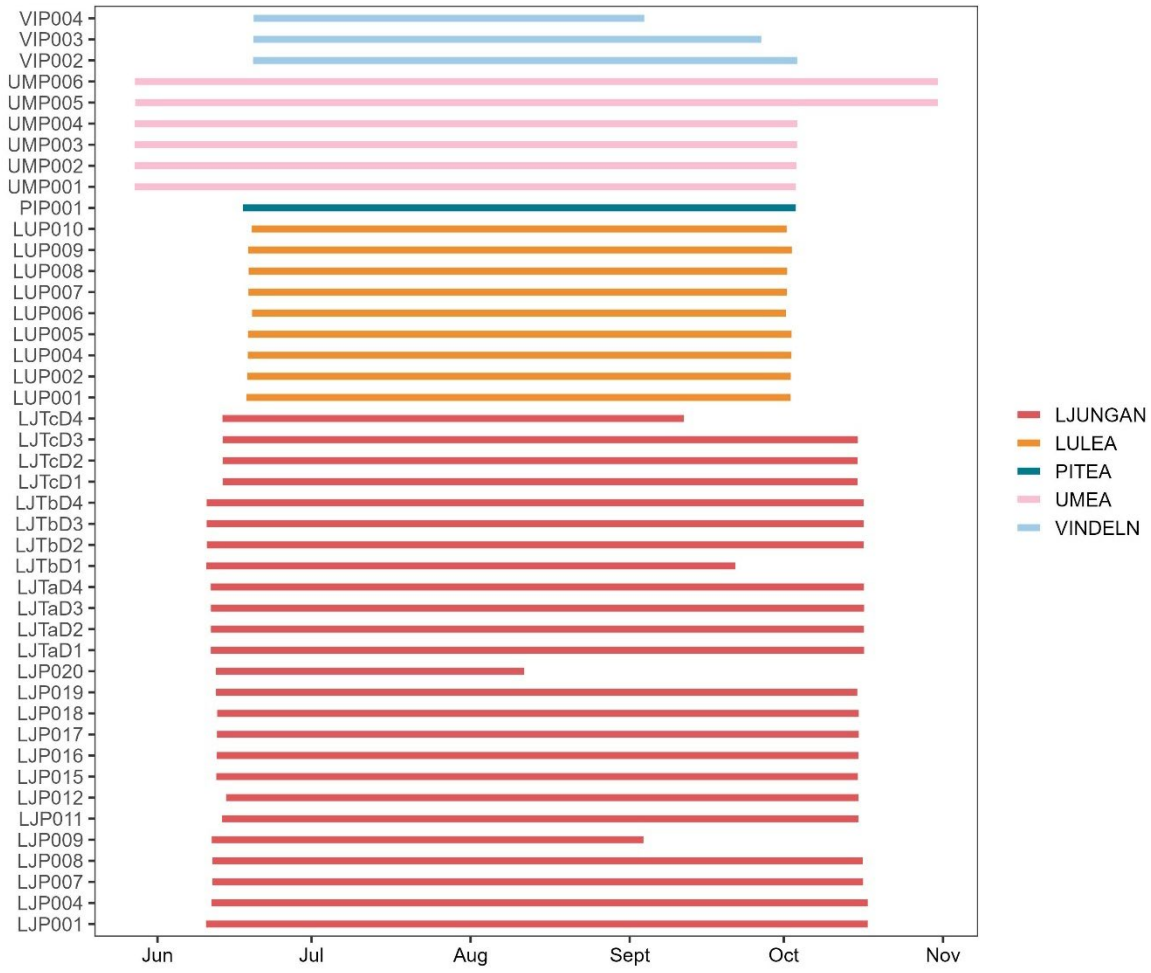

Figure 22: Logger activity bar plot showing raw timespan of the monitoring period June-October 2024 is Sweden.

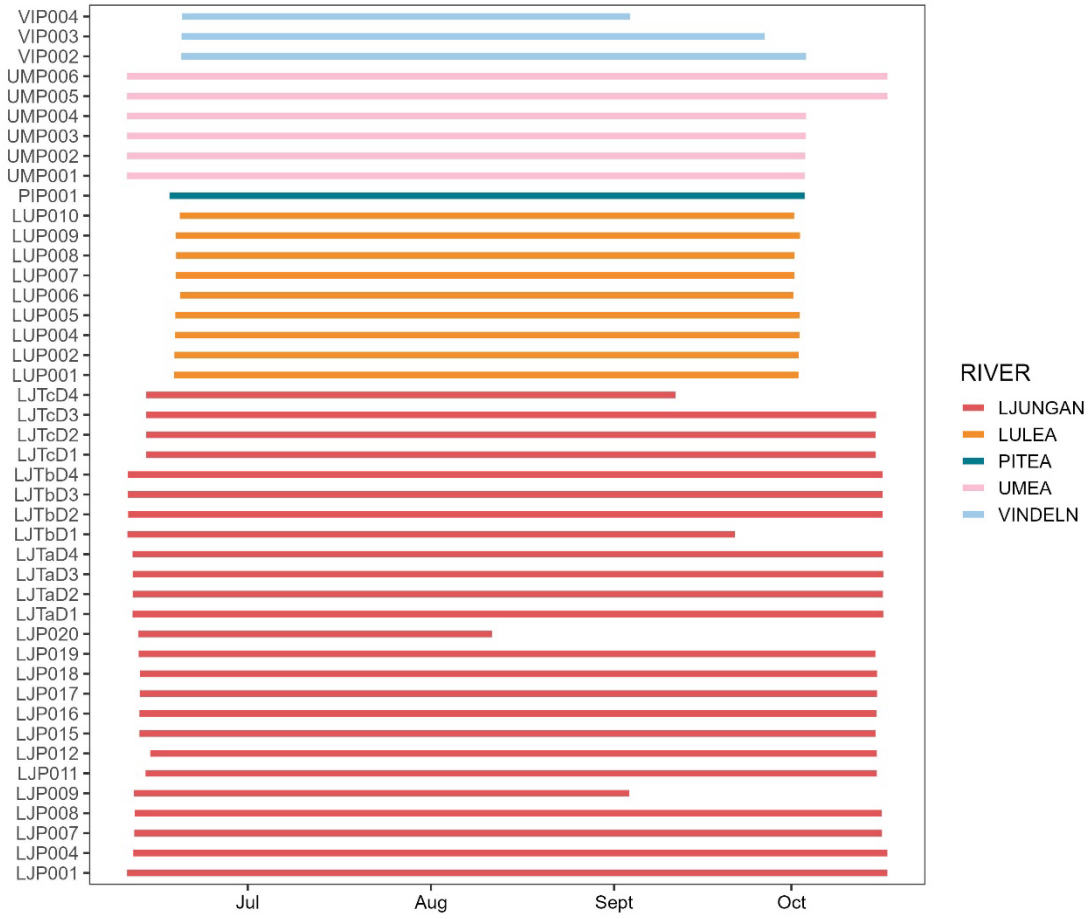

Figure 23: Logger activity bar plot showing clipped timespan of the monitoring period June-October 2024 is Sweden.

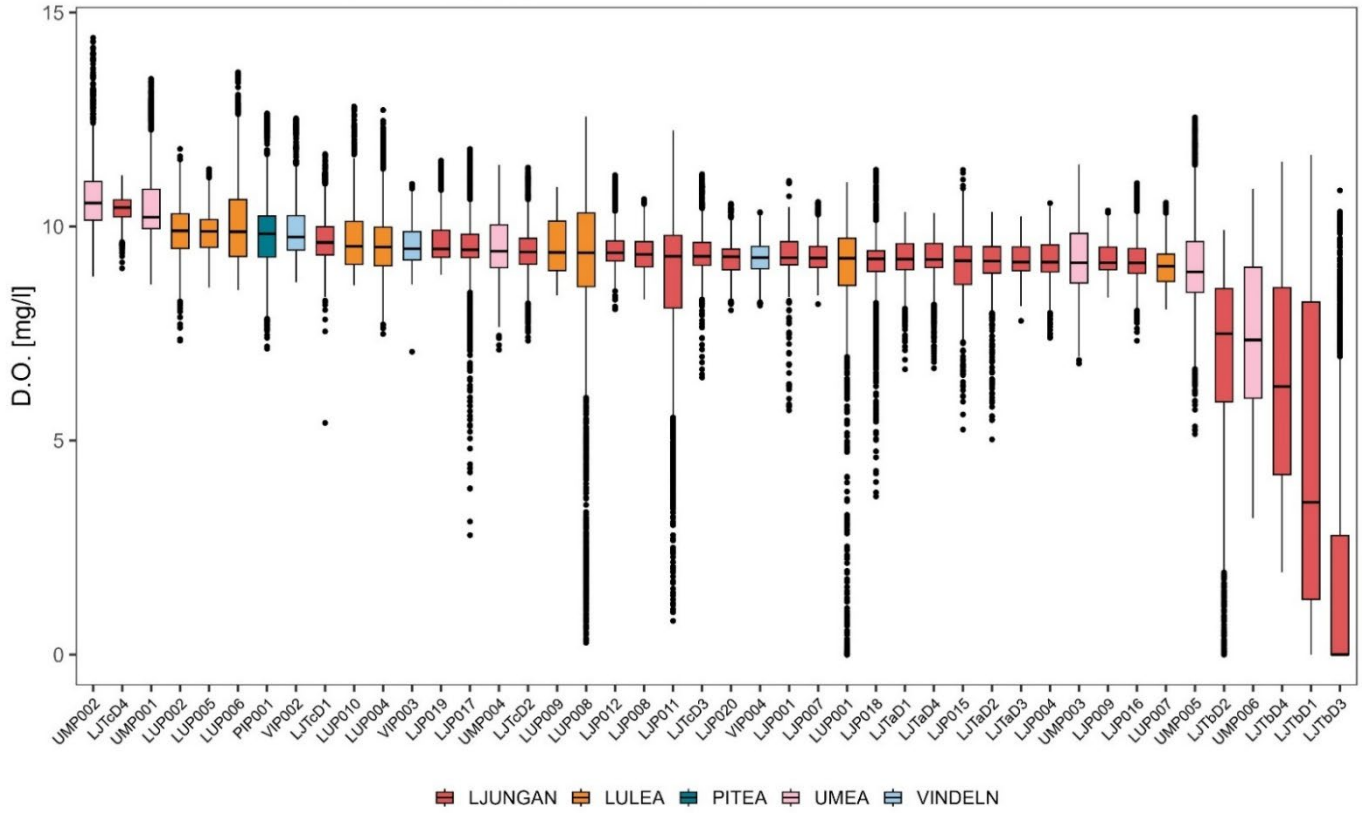

Figure 24: Variation of dissolved oxygen (DO) by Logger ID, row data relative to the study period June-October 2024. Boxplots display the distribution of DO measurements in mg/l collected in different locations. Each box represents one logger (ID), showing median, interquartile range (IQR), whiskers (showing minim and maximum without outliers) and extremes. Part of the extremes were removed as explained in the data cleaning section of the supplementary methods.

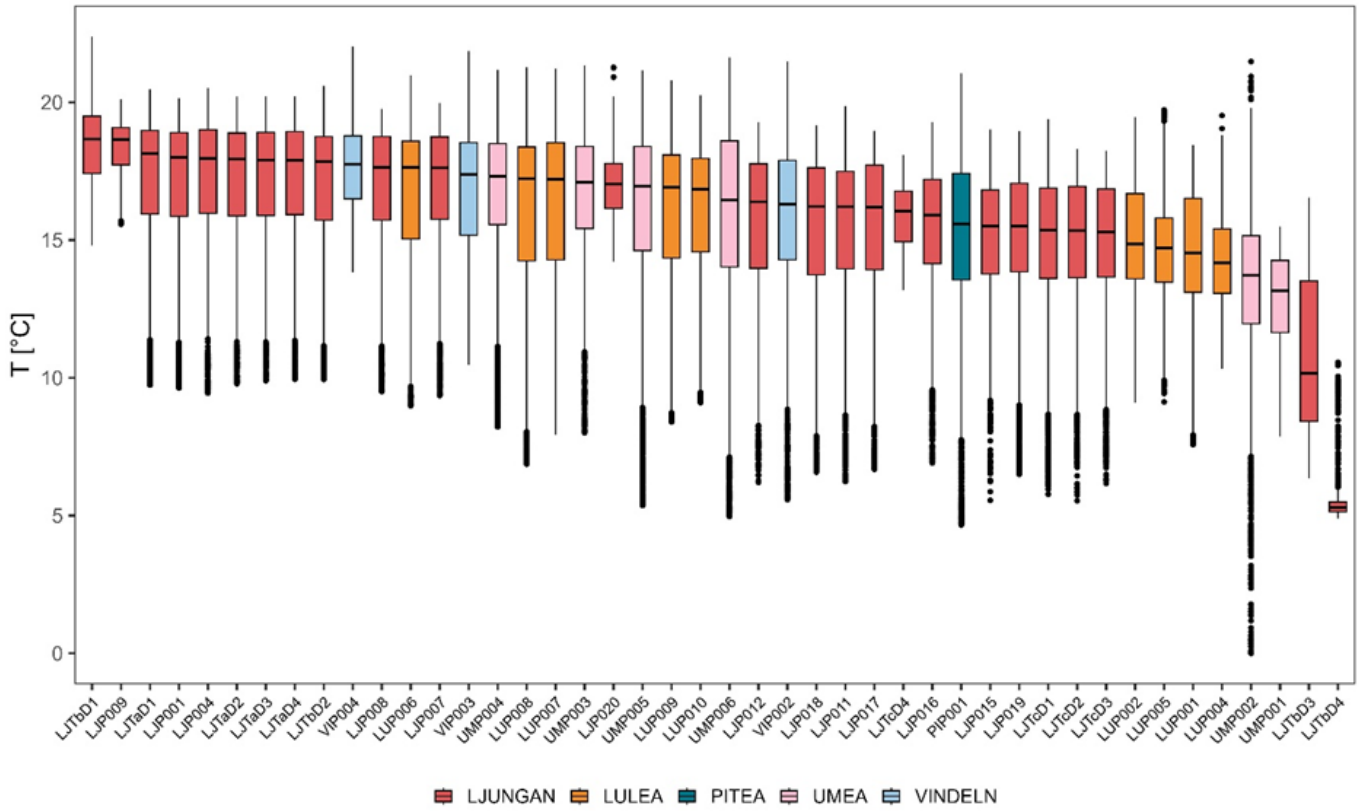

Figure 25: Variation of Temperature by Logger ID, row data relative to the study period June-October 2024. Boxplots display the distribution of DO measurements in mg/l collected in different locations. Each box represents one logger (ID), showing median, interquartile range (IQR), whiskers (showing minim and maximum without outliers) and extremes.

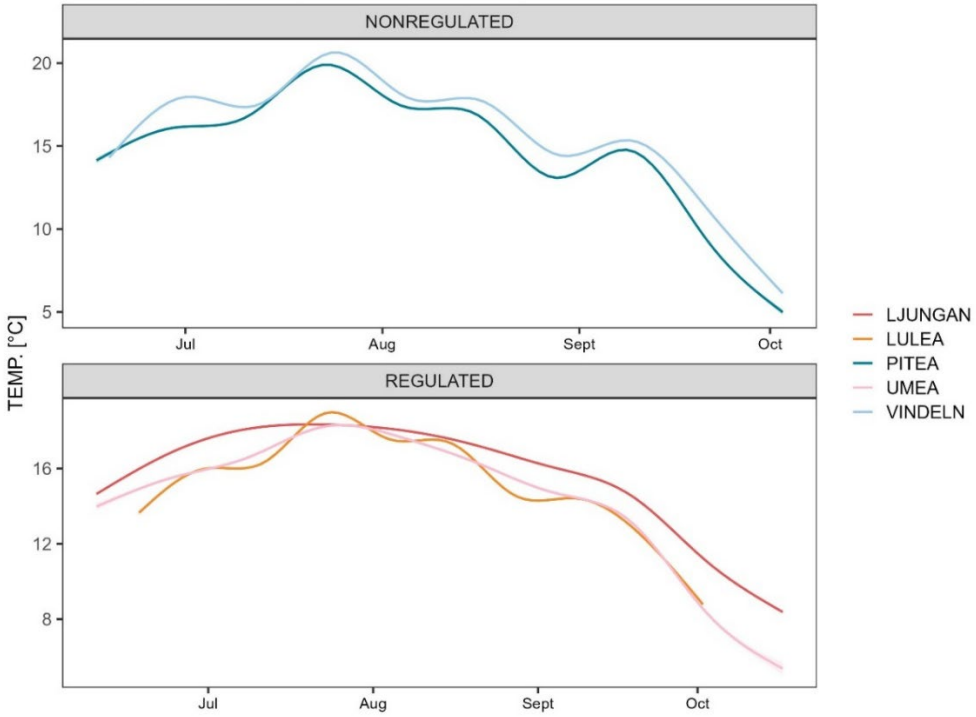

Figure 26: Temporal variation of water temperature across selected rivers in Sweden. Smoothed trend lines (GAMs) show changes in water temperature [°C] over the study period June-October. Shaded areas represent 95% confidence interval

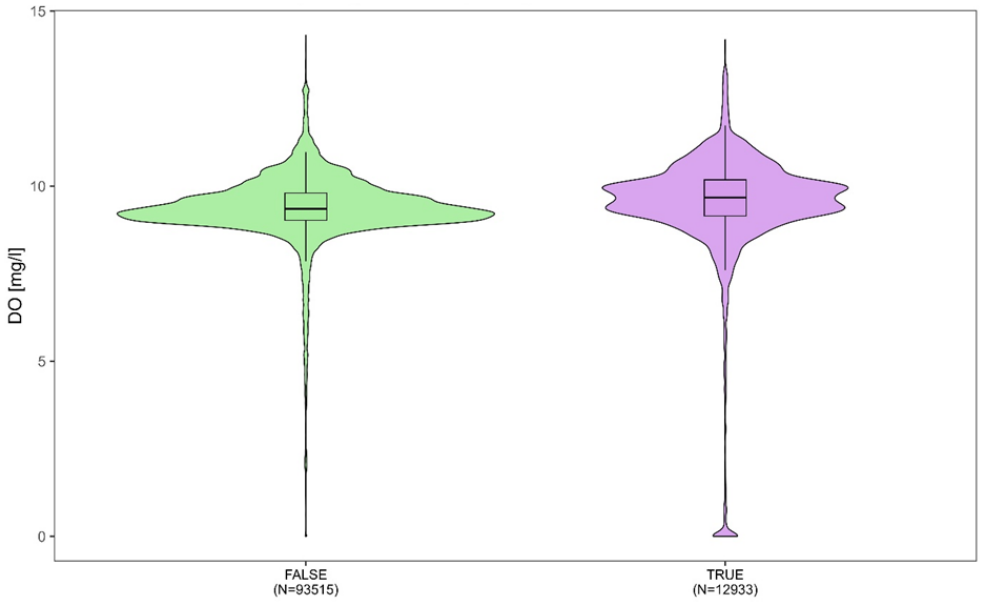

Figure 27: Distribution of dissolved oxygen (DO) in relation to zero flow condition. Violin plots show the distribution of DO measurements mg/l during zero-flow events (True) and with flowing water (False) highlighting differences in DO availability under different hydrological conditions. The data cover the study period June - October 2024 in Swede

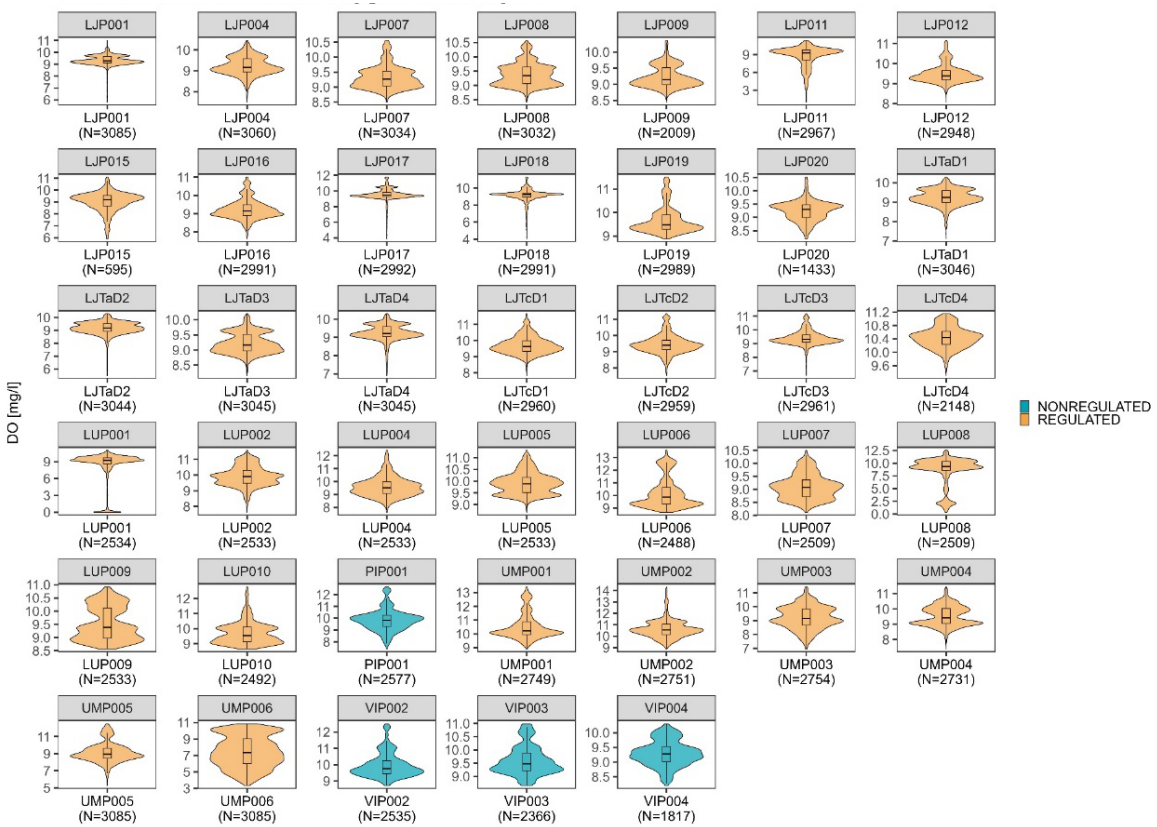

Figure 28: Distribution of dissolved oxygen (DO) across selected depth classes 0-3m, 3-6m, 6-9m and <9m. Violin plots show the distribution of DO measurements in mg/l. The inner boxplots represent the median, interquartile range (IQR), whiskers (showing minim and maximum without outliers). Data are relative to the study period June-October 2024 in Sweden.

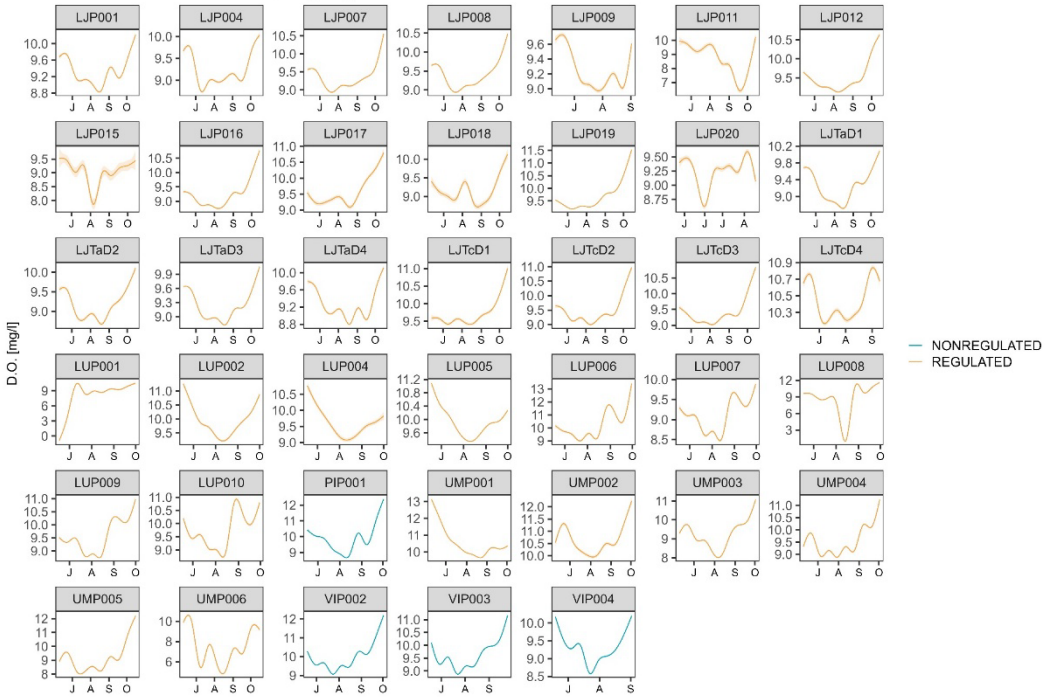

Figure 29: Temporal variation of dissolved oxygen (DO) across location in Sweden. Smoothed trend lines (GAMs) show changes in DO measurements [mg/l] of different loggers (ID) over the study period June-October 2024. Shaded areas represent 95% confidence interval

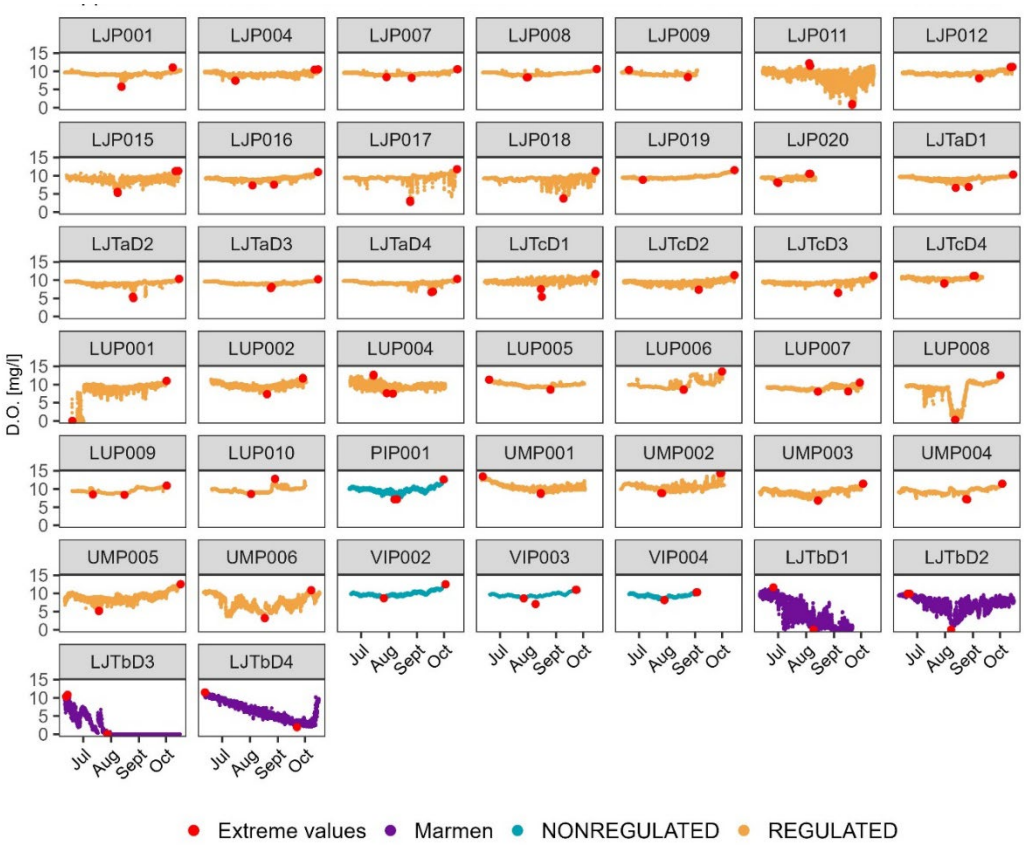

Figure 30: Scatterplot of raw dissolved oxygen (DO) measurements across ID and regulation classes. The plot shows raw DO measurements over time, grouped by location (ID). Data points are coloured by regulation class, allowing visual comparison between regulated and non-regulated rivers. Purple dots (Marmen) indicate non-representative data that were excluded from analysis, while red dots (Extremes) represent extreme values removed during the data cleaning process.

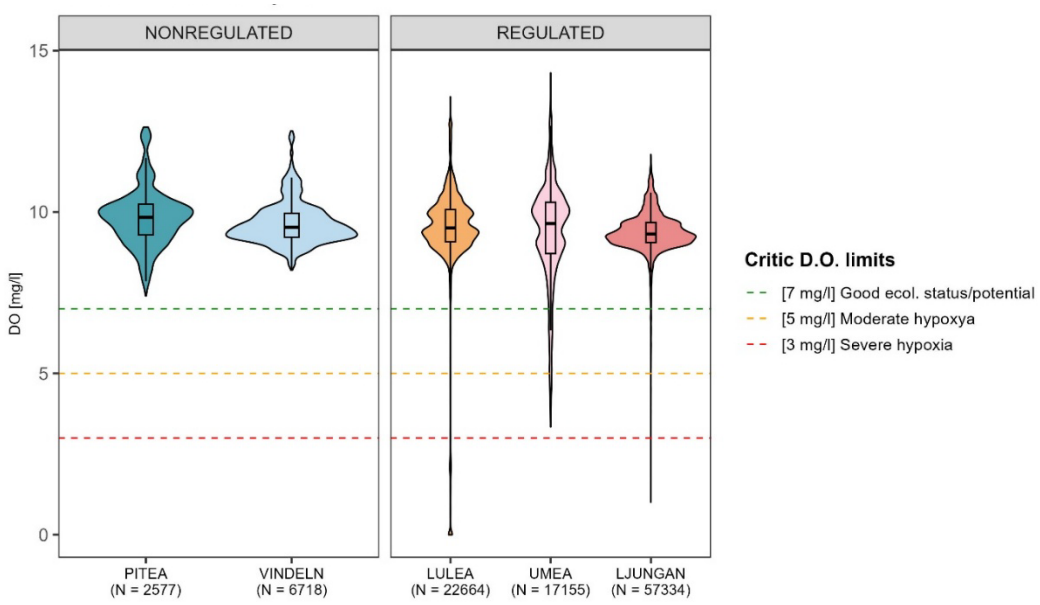

Figure 31: Distribution of dissolved oxygen (DO) across selected rivers by regulation class. Violin plots show the distribution of DO measurements in mg/l relative to each river. The inner boxplots represent the median interquartile range (IQR), and whiskers (showing minim and maximum without outliers). Horizontal reference lines indicate ecologically relevant thresholds: 7mg/l (minimum for good ecological status), 5 mg/l (moderate hypoxia), and 3 mg/l (severe hypoxia). Data are relative to the study period June-October 2024 in Sweden

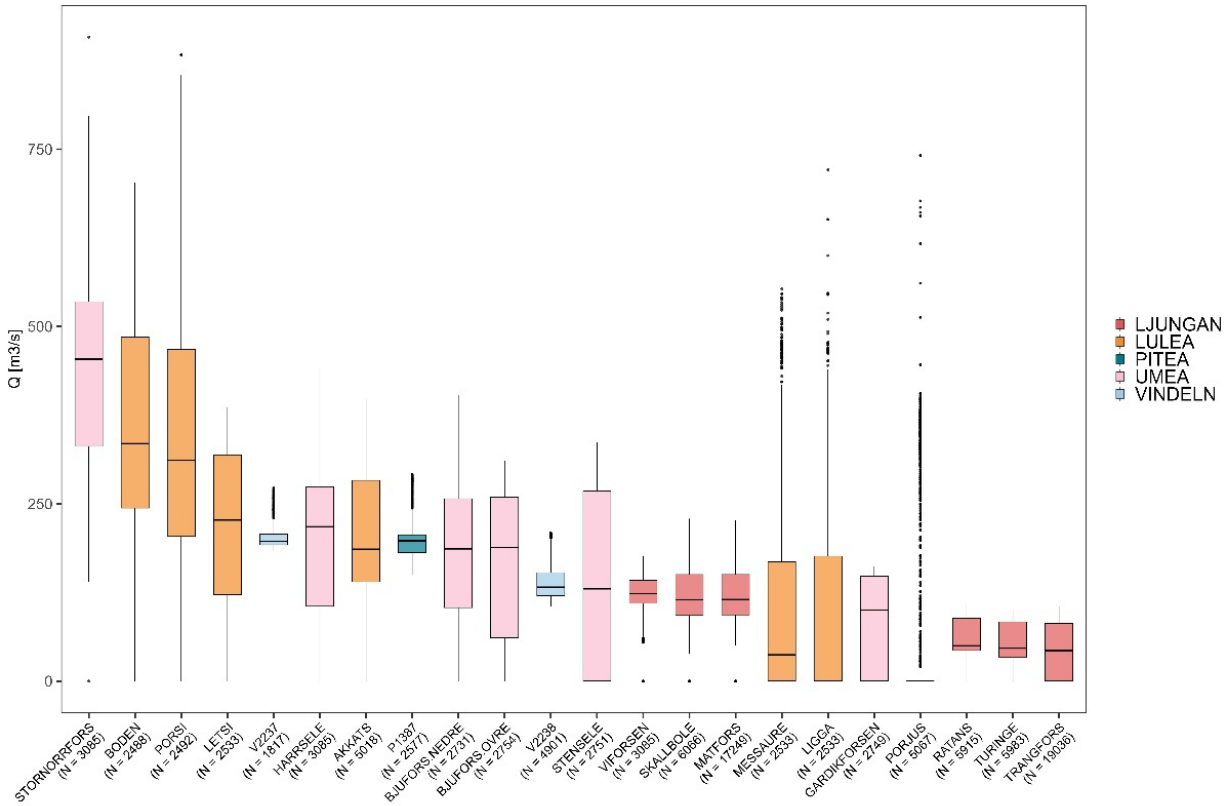

Figure 32: Variation in outlet discharge across hydropower stations (HP). Boxplots display the distribution of outlet discharge [m³/s] recorded at different HP stations. Each box represents one station, showing median, interquartile range (IQR), whiskers (showing minim and maximum without outliers) and extremes (which were not considered outliers).

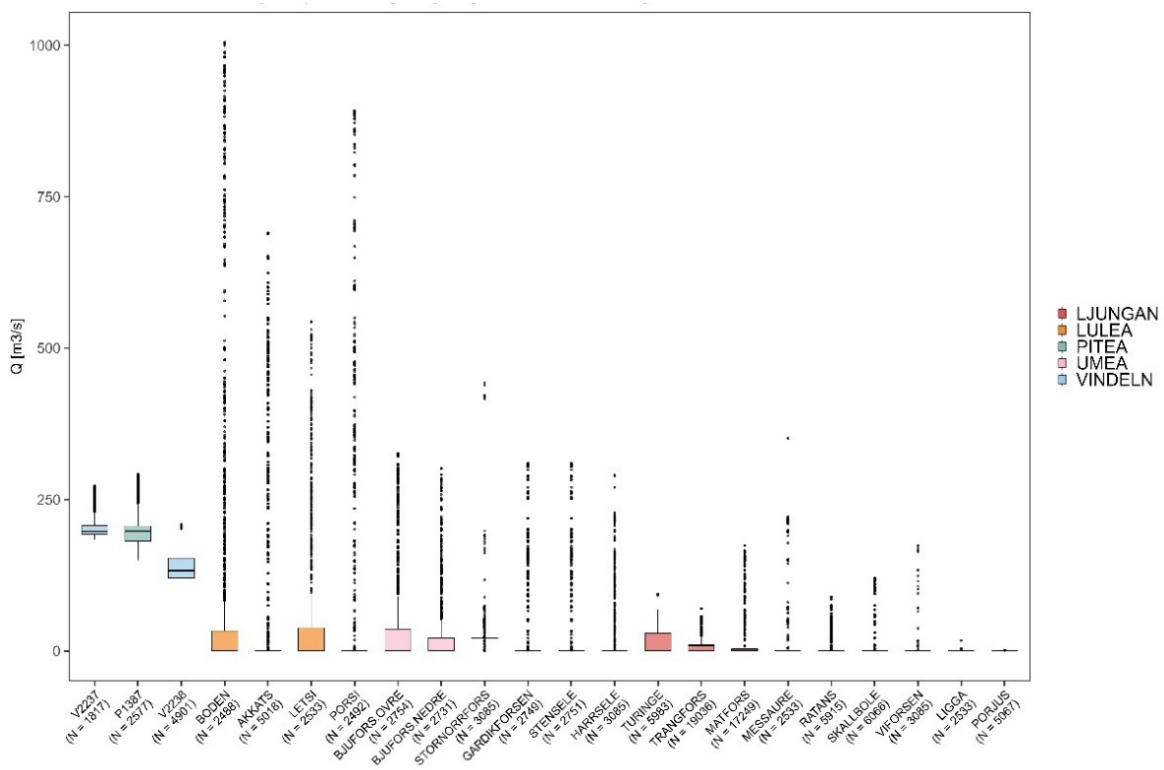

Figure 33: Variation in spill discharge across hydropower stations (HP). Boxplots display the distribution of spill discharge [m³/s] recorded at different HP stations. Each box represents one station, showing median, interquartile range (IQR), whiskers (showing minim and maximum without outliers) and extremes (which were not considered outliers).

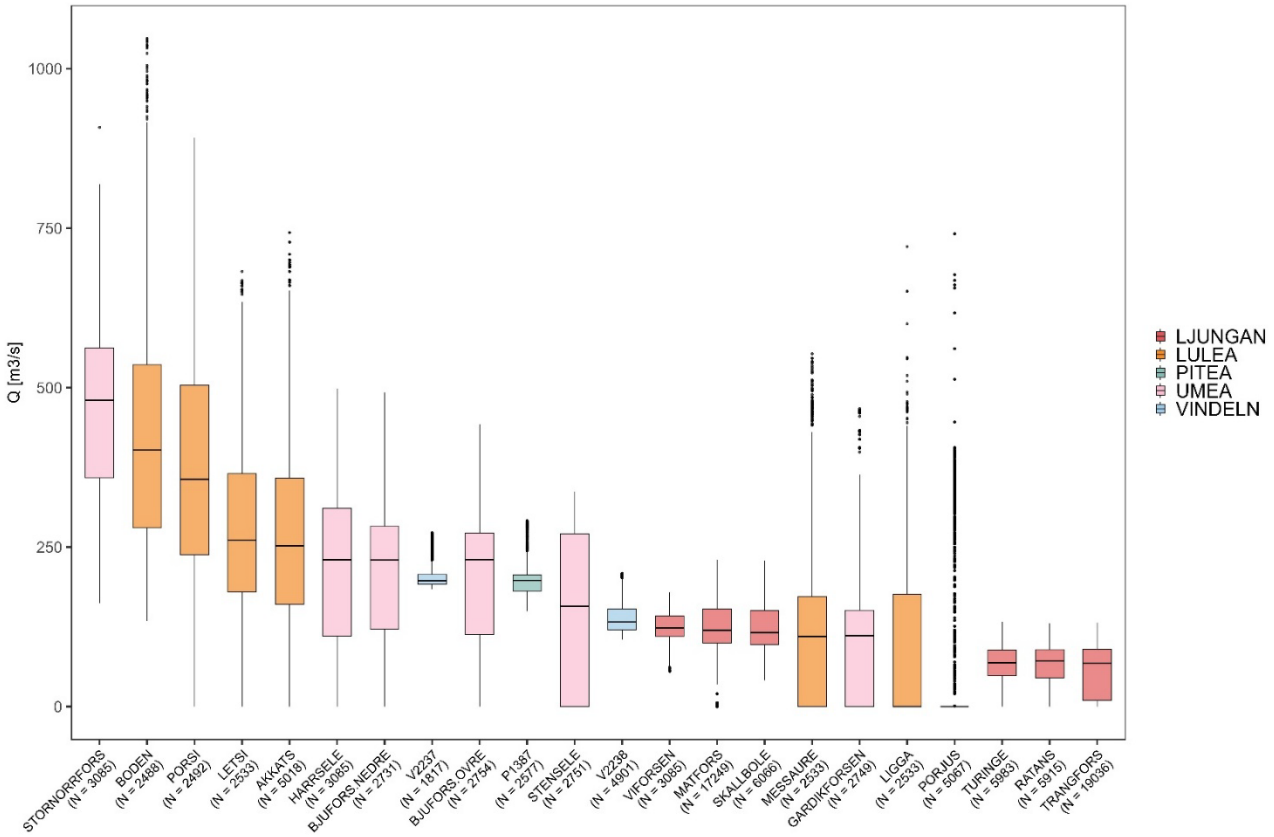

Figure 34: Variation in total discharge across hydropower stations (HP). Boxplots display the distribution of total discharge [m³/s] recorded at different HP stations. Each box represents one station, showing median, interquartile range (IQR), whiskers (showing minim and maximum without outliers) and extremes (which were not considered outliers).

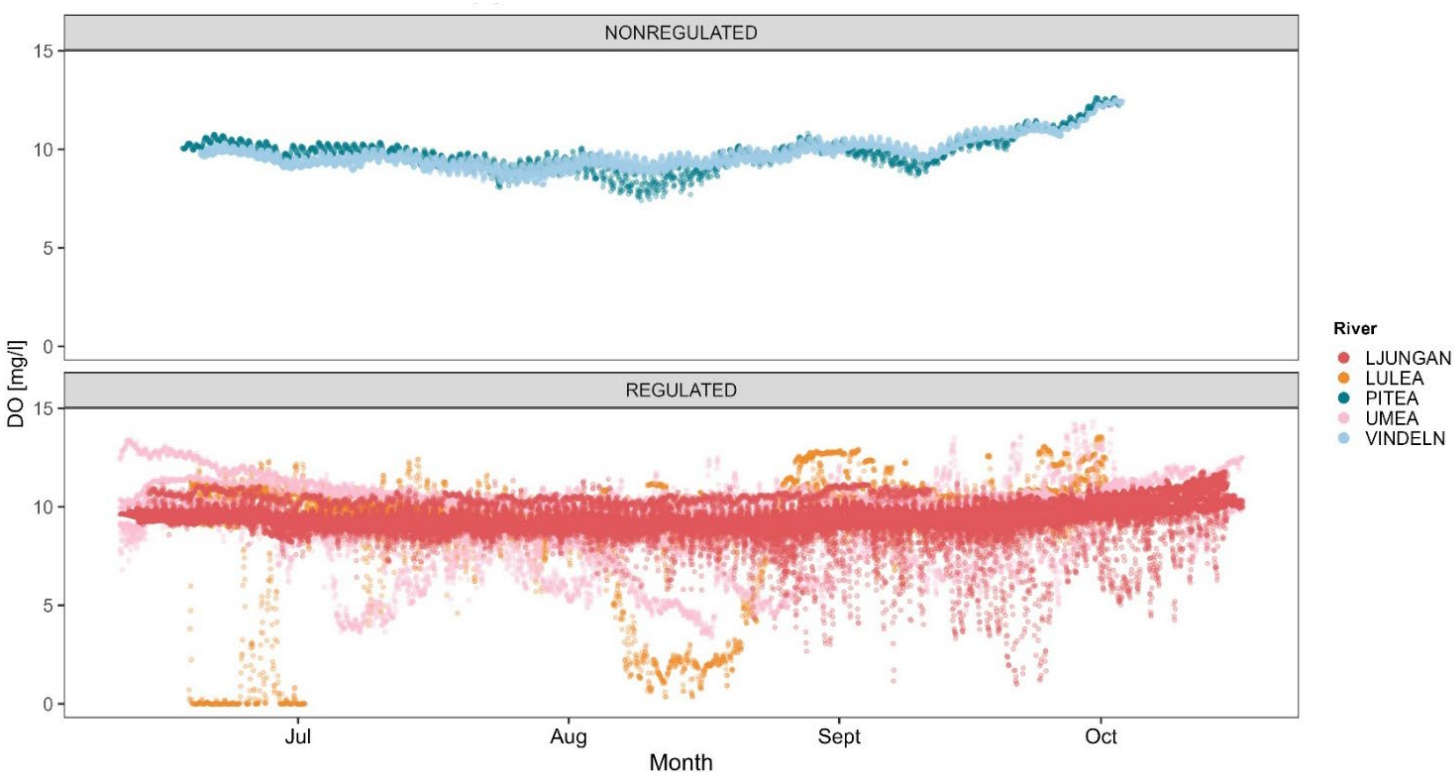

Figure 35: Scatterplot of dissolved oxygen (DO) measurements over time across selected rivers and regulation classes. The plot displays dissolved oxygen concentrations in mg/l measured over time rendered by river. Each point represents a single observation, enabling visual assessment of temporal trends and variability in DO across different rivers and regulation class. The plot also underlines the much higher temporal variability of DO in regulated rivers during the study period June-October in Sweden.

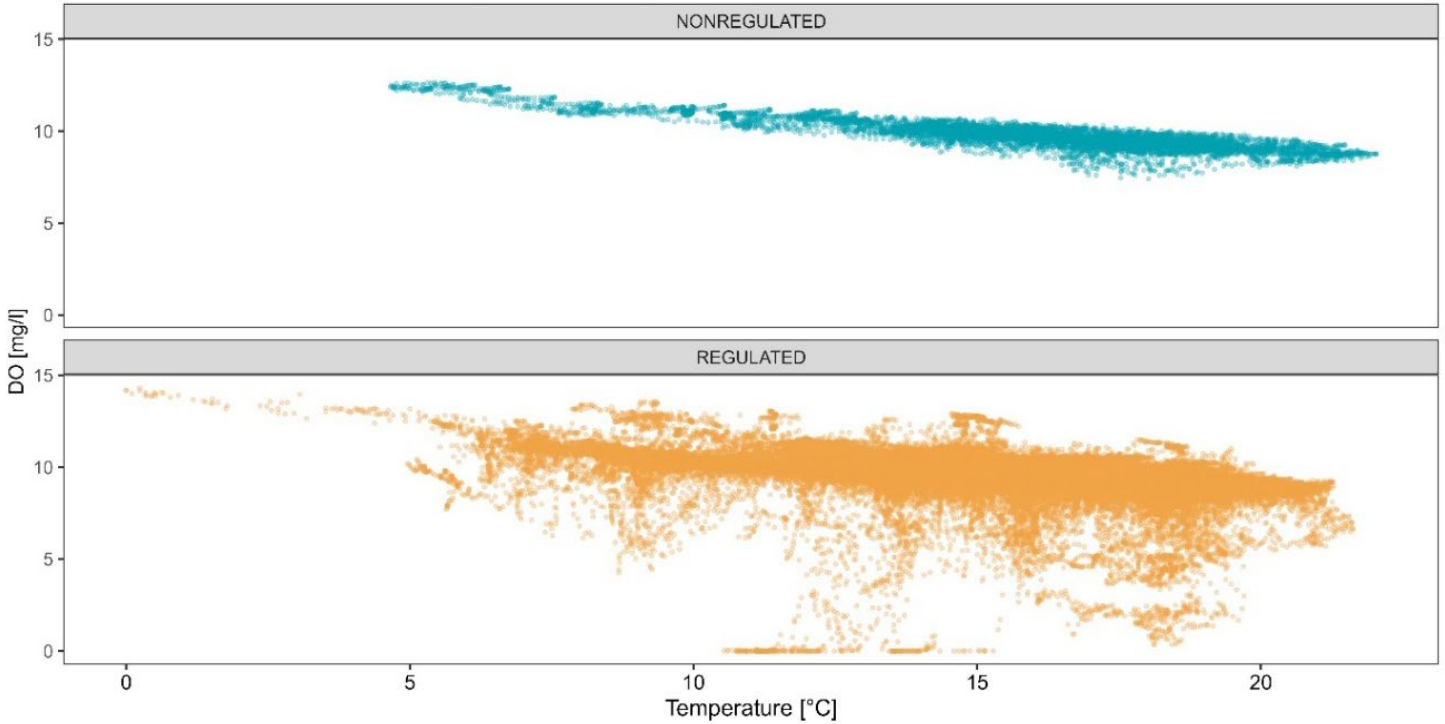

Figure 36: Scatterplot of dissolved oxygen (DO) in relation to temperature by regulation class. The plot displays dissolved oxygen concentrations [mg/l] on the y-axis against water temperature [°C] on the x-axis, with points coloured by regulation class (regulated vs. non-regulated). Each point represents a single observation, enabling visual assessment of the relationship between temperature and DO. The plot also allows comparison of the strength of this relationship between regulated and non-regulated rivers during the study period June-October in Sweden.

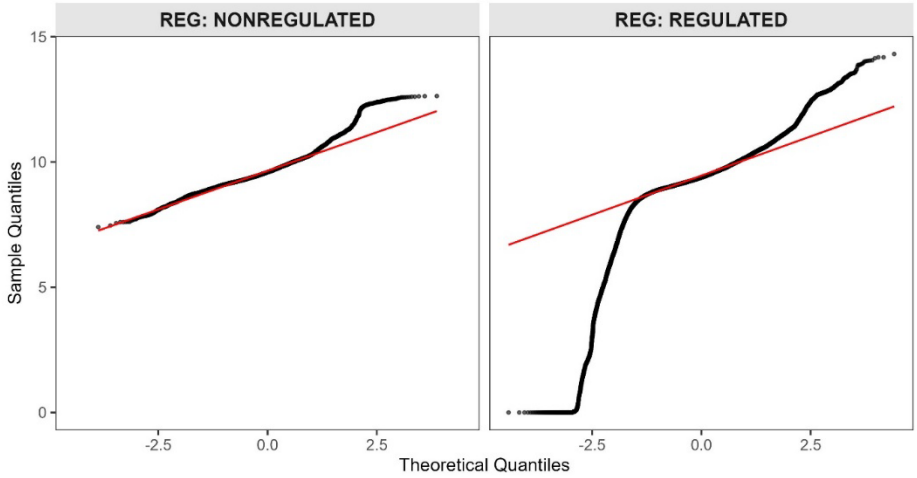

Figure 37: Q-Q plot of residuals by regulation class for normality check. Quantile–Quantile (Q-Q) plots display the distribution of residuals, divided by regulation class (regulated vs. non-regulated). The plot was obtained using stat_qq() function from ggplot2 R package to further assess normality of the distribution. Deviations from the reference line (red) indicate drift from a normal distribution.

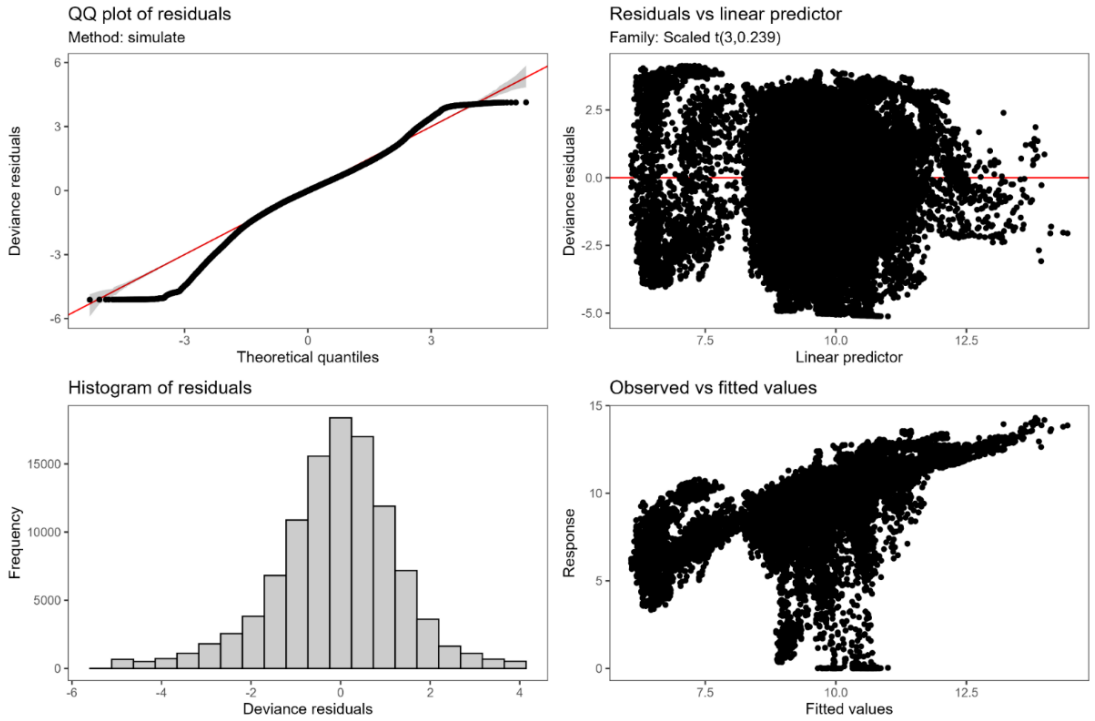

Figure 38: Residuals diagnostics for the final GAM model using a scaled t-distribution. Diagnostic plots generated using check.gam() for the final generalized additive model (GAM) fitted with a scaled t-distribution family. Panel 1 (up-left) shows a Q-Q plot assessing the normality of residuals; Panel 2 (up-right) displays residuals vs the linear predictor to evaluate homoscedasticity; Panel 3 (down-left) presents a histogram of residuals to inspect their distribution; and Panel 4 (down-right) plots observed vs fitted value

Supplementary methods

Merging details

The merging procedure consisted of two main steps. First, 45 temporary datasets were created by merging each logger's data with its corresponding upstream hydropower plant flow data. Second, all temporary datasets were combined into a single dataset.

Each provisional dataset was generated by filtering logger data by ID from the "all loggers" dataset, formatting the date-time column (as previously described), and renaming it to "Date." Corresponding flow data were filtered by "Powerplant ID" from the "Flow" dataset. Using *left_join()*, the two datasets were merged by "Date" and "Powerplant ID." After verifying column names, all 45 temporary datasets were combined into a single "oxygen-flow dataset" using *rbind()*. This final dataset included data from 19 hydropower plants and 3 SMHI stations, covering 45 loggers.

The dataset was then checked for missing values, revealing 1,054 rows with NAs in five columns. Further inspection showed that these were related to three loggers in Umeälven: UMP004, UMP005, and UMP006. The 24 missing values in UMP004 were due to absent *Spill flow* entries in the original dataset for Bjufors Nedre, which also affected *Total flow*, *Zero flow*, and *Total zero flow*. The remaining 1,030 missing rows were from UMP005 and UMP006, caused by a temporal mismatch: these loggers remained active until 21-11-2024, while flow data were only available up to 31-10-2024. All missing rows were removed using *na.omit()*.

Data cleaning

The activity time of each logger in the merged "oxygen-flow dataset" was visualized using *geom_line()* to display the individual data timespans (Figure 23). Since the merging process clipped flow data to match logger duration, the rendered timespans represented both data sources.

The maximum survey duration was 157 days (2024-05-27 13:00:00 to 2024-10-31 00:00:00), but loggers in Umeälven extended beyond this range. To prevent overrepresentation and reduce influence on model extremes, the dataset was clipped by excluding UMP001–UMP006, resulting in a uniform survey window of 129 days (2024-06-10 11:00:00 to 2024-10-17 09:00:00).

To improve data quality, the first and last two hours of measurements for each ID were removed to avoid data potentially collected out of water. The final clipped survey period was 2024-06-10 14:00:00 to 2024-10-17 06:00:00, yielding 118,277 observations. A post-clipping activity plot was then generated (Figure 24).

Next, DO distribution was assessed using *geom_boxplot()* (Figure 25), revealing a high number of extreme values beyond whisker limits. These were retained, as they likely reflected real environmental variability. However, to remain conservative, the two highest and two lowest DO values per logger were extracted and visualized using *geom_point()* (Figure 31), then removed.

Additionally, the LJTb transect (Marmen) displayed anomalously wide variability and violated key protocol assumptions due to suboptimal deployment location. Loggers LJTbD1-LJTbD4 were therefore excluded, removing 11,653 observations.

Combined, the removal of extreme values and non-representative loggers eliminated 17,829 observations. Along with previous steps, the cleaning process removed 18,751 records -approximately 15% of the raw “all loggers” dataset- resulting in the final “model dataset” with 106,448 rows and 20 columns, which was exported as a CSV file.

Publishing and archiving

Approved students' theses at SLU can be published online. As a student you own the copyright to your work and in such cases, you need to approve the publication. In connection with your approval of publication, SLU will process your personal data (name) to make the work searchable on the internet. You can revoke your consent at any time by contacting the library.

Even if you choose not to publish the work or if you revoke your approval, the thesis will be archived digitally according to archive legislation.

You will find links to SLU's publication agreement and SLU's processing of personal data and your rights on this page:

- https://libanswers.slu.se/en/faq/228318
-

☒ YES, I, Marco Cunico, have read and agree to the agreement for publication and the personal data processing that takes place in connection with this.

☐ NO, I/we do not give my/our permission to publish the full text of this work. However, the work will be uploaded for archiving and the metadata and summary will be visible and searchable.